International Journal of Nanomedicine

Dovepress
open access to scientific and medical research

Open Access Full Text Article

REVIEW

How Magnetic Composites are Effective Anticancer Therapeutics? A Comprehensive Review of the Literature

Mostafa Yusefi[1,2], Kamyar Shameli[3], Hossein Jahangirian[4], Sin-Yeang Teow[5], Leili Afsah-Hejri[6], Siti Nur Amalina Mohamad Sukri[1], Kamil Kuča[1,7,8]

[1]Malaysia-Japan International Institute of Technology, Universiti Teknologi Malaysia, Kuala Lumpur, Malaysia; [2]Institute of Biological Sciences, Faculty of Science, Universiti Malaya, Kuala Lumpur, 50603, Malaysia; [3]Institute of Virology, School of Medicine, Technical University of Munich, Munich, 81675, Germany; [4]CaroGen Corporation, Farmington, CT, USA; [5]Department of Biology, College of Science, Mathematics and Technology, Wenzhou-Kean University, Wenzhou, Zhejiang Province, 325060, People's Republic of China; [6]Department of Food Safety and Quality, School of Business, Science and Technology, Lakeland University Plymouth, WI 53073, USA; [7]Department of Chemistry, Faculty of Science, University of Hradec Kralove, Hradec Kralove, Czech Republic; [8]Biomedical Research Center, University Hospital Hradec Kralove, Hradec Kralove, Czech Republic

Correspondence: Kamyar Shameli; Hossein Jahangirian, Tel +4917646555701; +16178608429, Email kamyarshameli@gmail.com; kamran.jahangirian@gmail.com

Abstract: Chemotherapy is the most prominent route in cancer therapy for prolonging the lifespan of cancer patients. However, its non-target specificity and the resulting off-target cytotoxicities have been reported. Recent in vitro and in vivo studies using magnetic nanocomposites (MNCs) for magnetothermal chemotherapy may potentially improve the therapeutic outcome by increasing the target selectivity. In this review, magnetic hyperthermia therapy and magnetic targeting using drug-loaded MNCs are revisited, focusing on magnetism, the fabrication and structures of magnetic nanoparticles, surface modifications, biocompatible coating, shape, size, and other important physicochemical properties of MNCs, along with the parameters of the hyperthermia therapy and external magnetic field. Due to the limited drug-loading capacity and low biocompatibility, the use of magnetic nanoparticles (MNPs) as drug delivery system has lost traction. In contrast, MNCs show higher biocompatibility, multifunctional physicochemical properties, high drug encapsulation, and multi-stages of controlled release for localized synergistic chemo-thermotherapy. Further, combining various forms of magnetic cores and pH-sensitive coating agents can generate a more robust pH, magneto, and thermo-responsive drug delivery system. Thus, MNCs are ideal candidate as smart and remotely guided drug delivery system due to a) their magneto effects and guide-ability by the external magnetic fields, b) on-demand drug release performance, and c) thermo-chemosensitization under an applied alternating magnetic field where the tumor is selectively incinerated without harming surrounding non-tumor tissues. Given the important effects of synthesis methods, surface modifications, and coating of MNCs on their anticancer properties, we reviewed the most recent studies on magnetic hyperthermia, targeted drug delivery systems in cancer therapy, and magnetothermal chemotherapy to provide insights on the current development of MNC-based anticancer nanocarrier.

Keywords: magnetic nanoparticles, polymer-based magnetic nanocomposites, hyperthermia, external magnetic field, targeted cancer treatments

Introduction

Insights into advanced materials have eminently illuminated several authentic features for medical applications in the past few years to promote a healthy society. Specifically, fascinating and enlightening studies on novel therapies and magnetic nanocomposites (MNCs) are prone to offer solutions for many global health issues including cancer. In a practical example, the treatment of glioblastoma cancer by magnetic hyperthermia therapy (MHT) using magnetic nanoparticles (MNPs) has been approved in Europe.[1] Although MNPs alone have shown some merits in MHT and targeted anticancer drug delivery systems, they have several downsides such as colloidal instability, fast oxidation or sensitivity to air and humidity, self-agglomeration due to dipole–dipole attractions between the bare nanoparticles (NPs), low biocompatibility, undesired biodegradability, low drug encapsulation efficiency, and rapid drug release

Received: 31 May 2022
Accepted: 31 May 2023
Published: 30 June 2023

performance.[2,3] For these reasons, MNPs alone are relatively basic and essential, but not appropriate materials for enhanced pharmaceutical effects in drug delivery systems. To overcome these issues, MNCs with multifunctional counterparts and properties have been widely used in MHT and drug delivery to obtain localized synergistic chemothermotherapy.[4,5]

The non-targeted actions of high-dose chemodrugs (such as doxorubicin (DOX) and 5-fluorouracil (5FU)) can cause unwanted side effects.[6] The Food and Drug Administration (FDA) has already approved five nano-carriers, including inulin, alginate, liposomes, albumin NPs, and polymeric micelles.[7,8] These polymers are pH-sensitive, biocompatible, and biodegradable, which makes them suitable to be incorporated in novel nanotherapies.[9–11] In addition, biocompatible polymers can potentially be naturally eliminated from the body, because of their enzymatic degradation by colonic microbial agents.[12,13] However, polymers with single-modality function (eg, their pH-sensitive structure) are inefficient for multi-stage and targeted cancer treatments; since pH changes in the human body take a long time.[14,15] Incorporating biocompatible polymer in MNCs to fabricate polymer-based magnetic nanocomposites (PMNCs) will result in multi-functional and magnetized polymer structures with the ability to overcome challenges that lie ahead for the multi-stimulus responsive drug nanocarrier systems, MHT, and magnetic targeting.[16] Another factor is determination of the appropriate dosage of administered chemodrug to improve tumor drug uptake and avoid the dose-limiting toxicity. Therefore, development of external-stimuli responsive drug delivery systems by combining chemotherapy, MHT, and magnetic targeting can be used in order to reduce off-target toxicity of the applied drug and subsequently enhance the delivery of sufficient drug dosage to the target tumor with precise accumulation of MNCs onto the heated tumor area. This reflects that MNCs and PMNCs as low-cost and smart nanocarrier systems have gained tremendous attention in remote controllability and magnetothermally assisted drug release. This is due to their excellent structural properties including pH, thermo, and magneto-responsive along with high magnetization, colloidal stability, drug-conjugation, biodegradability, and biocompatibility manner.[4,17,18] In this manner, MNCs have been studied for MHT,[19–23] targeted drug delivery,[24,25] bioseparation,[26,27] biosensing,[28,29] cell labeling,[30] targeting and immunoassays,[31–33] targeted cancer therapy,[34,35] and magnetic resonance imaging (MRI).[36–39]

In an ideal scenario of chemothermotherapy using MHT, alternating magnetic field (AMF) can generate local heating onto MNCs and also tumor cells for thermal treatment and also a heat-dependent release of drug to sensitize cancer cells.[7] Improving the heat efficiency in MHT is not only related to externally applied parameters such as AMF and field frequency/amplitude but also attributed to the internal factors, including the type of the cancer cells and concentration, surface modification, morphology, viscosity, magnetic susceptibility/saturation magnetization, the average carrier alignment, size, shape, and nanostructure of MNCs. Another clinically related feature in MHT is the influence of intratumorally produced temperature on the blood flow within the tumor and the surrounding normal cells that a rise in temperature causes blood vessel dilation and subsequent enhancement of the permeability of vascular walls. In reality, the therapeutic benefit of hyperthermia on cancer has multiple causes, including but not limited to enhancement of drug absorption and cytotoxicity, greater sensitivity to radiation, and probably even more important, immunomodulation; generation of heat-shock proteins during hyperthermia can also play roles.

It should be mentioned that MHT alone cannot guide the injected MNCs in different areas of the human body, which is potentially addressed by using an external magnetic field (EMF) to steer and localize MNCs onto the targeted tumor tissue. EMF also reduces the possibility of obstruction in blood vessels and obtains extended retention once the particles are injected into tumor tissues to enhance the accumulation of MNCs for an effective inflammation procedure. Further, EMF can be used to remove MNCs from the tumor tissue. It is highly suggested to remove the administered MNCs from the body after their oxidative damage and cancer-killing effects[40] since the MNCs might penetrate the blood–brain barrier and generate the iron disbalance in the body causing Alzheimer's[41] and Parkinson's disease.[42] An important challenge is declining the effects of AMF and EMF with distance to appropriately heat and guide the administered MNCs.[43] Thus, it is vital to overcome the mentioned issues in order to use MNCs in combination with hyperthermia and targeted cancer therapy as the cornerstone of the nanodrug delivery systems and localized cancer treatments.

Several studies have been devoted to reviewing the use of various MNCs for the development of MHT[44] and smart drug delivery systems.[45–49] However, there have been no comprehensive reviews on fabrication methods, properties of MNPs as well as drug-loaded MNCs for magnetothermal chemotherapy using MHT and magnetic targeting, in which this

study was conducted. As the main objective of this review paper, it is vital to build a bridge between the physicochemical properties of MNCs and a promising strategy of stimulus-triggered drug delivery via incorporating diagnostic and therapeutic agents into a single biocompatible nanoplatform. The purpose of this review article is to minutely discuss the structure of magnetism and different synthesis methods and surface modifications of MNCs for drug delivery systems, MHT, as well as magnetic targeted cancer therapy. This paper mainly focuses on the recent articles with respect to development and interests within the key parameters of synthesis of MNCs for the pH-responsive and magnetothermal-facilitated drug release, heat treatment, and targeted cancer therapy.

Investigation of Magnetic Properties

MNPs are essential counterparts of MNCs. They can be classified into magnetic alloy NPs (eg iron, nickel, and cobalt) and magnetic metal oxide NPs (eg iron oxides, nickel oxide, and lanthanum strontium manganite). Magnetic nano-agents such as ferromagnets (FM) and ferrimagnets (FiM) have potent molecular exchange interactions with the ability to produce a magnetization. Permanent magnets are the well-known FM and FiM, which are not limited to a submicroscopic scale. A material acts as an FM when the exchange interactions between atoms set off magnetic moments in order to support one another, and analogous orientation of magnetic moments would arise below a critical temperature known as Curie temperature (Tc).[50] A material performs as a paramagnet beyond Tc where its magnetization disappears since thermal energy overcomes the exchange interaction. FiM performs similarly to FM with comparable Tc, quick and high magnetization, and hysteresis, although lower than FM upon EMF. Table 1 shows categories of magnetisms and their magnetic properties.

The Types of Magnetization Materials

FiM is a magnetic ordering that attributed to the metal ions and electron interactions as the magnetic moments with spontaneous alignment below Tc, causing the formation of magnetization.[44] The typical difference between FM and FiM (which was not differentiated from FM before 1948) is that the FiM materials consist of different types of atoms in the resulting magnet's unit cell. Without EMF, the lattice of FiM is a combination of two separate sub-lattices with varied strengths, non-parallel formation, and dissimilar magnetic moments where one direction has a stronger magnetic moment than others to obtain the net magnetization. FiM shows similar net magnetization and hysteresis to FM, nevertheless,

Table 1 Categories of Magnetism Materials and Their Characteristics

Type	Example, Refs	Net Magnetization	Response to EMF	Response After Removing EMF	Susceptibility
Diamagnetic	Au, Ag, and most of known elements, [51,52]	0	Weak response, aligned contrary to the applied EMF	Do not retention of magnetic moment	Very small and negative (−10-4 to −10-6)
Paramagnetic	Na, Mg, Al, Ga, Li, Ta, Cu,[53]	✓	Sectional response, aligned positive to the direction of EMF	No retention of magnetic moment	Small and positive (10–4 to 10–6)
FM	Fe, Co, Ni,[54]	✓	Potent response, aligned parallel to EMF	Remains a residual magnetic moment	Very large and positive (104 to 106)
Antiferromagnetic	MnO, CoO, NiO, CuCl2,[55]	0	Potent response, aligned parallel to EMF	A residual magnetic moment remains	Small and positive (0.1–1)
FiM	BaFe12O19 Fe_3O_4, $MnFe_2O_4$, Magnetite (Fe_3O_4) and maghemite (γ-Fe_2O_3),[56]	✓	Potent response, aligned parallel to EMF	A residual magnetic moment exists after the removal of EMF	Large and positive (103 to 105)

with opposite magnetic ordering and they become FM and paramagnets at below and above Tc, respectively. The FiM structure can be indicated in $MgFe_2O_4$[57], γ-Fe_2O_3[58], α-Fe_2O_3[59], $CoFe_2O_4$[60], and $MnFe_2O_4$.[61]

Transition metals of Fe, Ni, and Co and their alloys are the most well-known FM, indicating analogously oriented atomic magnetic moments and magnetic characteristics even after removal of EMF. In FM, the large electron exchange forces may lead to the potent exchange interactions among neighboring moments and the alignment of the two-electron spins with strong magnetizations. FM with small and large coercive fields (Hc) are such soft and hard magnetic materials, respectively. Compared to soft magnetic materials, the magnetization of hard magnetic materials desires more energy and subsequently a wider hysteresis loop. Magnetic responses of FM at below Tc order are aligned in the same direction and provoke the decrease of exchange energy of the material. FM particles maintain their spontaneous magnetization with aligned atoms in one direction without applied EMF. This is due to the lack of tendency in the electron field of FM' atoms.[62]

Superparamagnets have indicated a great potential in magnetic nanofluid hyperthermia treatment and targeted cancer therapy.[3,63] Above block temperature (which occurs just before TC)[64], both small nanosize of FM or FiM particles (20–100 nm) have a tendency of superparamagnetic behavior that the amount of domain walls for each particle decreases to only one wall with a single domain, due to low energy statement and the absence of boundaries. Superparamagnets obtain magnetization quicker than other forms of nanomagnetism, and each atomic magnetic moment preserves its ordered state, causing a non-hysteretic curve with zero Hc and remanent magnetization (Mr).[65]

In the periodic table, chromium is the only element as antiferromagnetism with a weak state of magnetism and positive susceptibility, and become paramagnets above Tc.[55] Diamagnetism is a common feature of all material resulting from the non-supportive performance of electrons in the presence of EMF. Without EMF exposure, diamagnetic materials exhibit zero magnetization (due to lack of orbital shells and unpaired electrons), whereas with EMF exposure, they show a negative magnetization. In a recently reported study,[51] EMF around the synthesis container could collect the magnetic iron particles, while diamagnetic Bismuth and gold NPs were successfully separated.[51]

The Synthesis of Magnetic Nanoparticles

Since 1996, the synthesis of MNPs with various physicochemical properties and morphologies has been widely carried out by several techniques based on chemical, physical, and green routes (Figure 1a).[66] Ferrous sulfate or iron(II) sulfate is an inorganic salt that can be utilized as precursor in the formation of iron compounds. For many years, the LaMer burst nucleation has been used to explain the procedure of the nucleation and development of NPs.[67,68] In 1950, LaMer and Dinegar declared a model for the mechanisms of nucleation-growth of sulfur particles related to the three phases (Figure 1b).[68] In the first stage, the metal salts were soluble in the homogeneous media than via increasing salt concentration, the reduction process of metallic NPs called nucleation (Cmin) starts. The continuous increase of the salt concentration leads to a certain critical supersaturation level (Cmax) since the molecules construct nuclei and the media becomes heterogeneous.[68] In the second stage, the nuclei is resulted from the collisions between ions and molecules of the media in an autonucleation procedure. In particular, the Cmax concentration of the metal salts declines quickly to Cmin because of the development of clusters, and then the amount of nucleation drops instantly to zero. In the third stage, the cluster steadily increases to form a critical size, while the cluster converts into a structure known as "seed". Lastly, the seed keeps growing to obtain a nanocrystal by enhancing metal atoms as the number of salts in the media declines to a solubility concentration of nanocrystals (Cs) and the NPs fabrication.[68,69] In MHT, MNPs are unique nano agents with magnetic properties, which is a basis of several advanced biomedical demands (Figure 1c).

Chemical Methods

The chemical co-precipitation method is widely applied in the synthesis of many different MNPs and MNCs, due to its low-cost, simple, and fast chemical route.[71] However, this method may result in low crystallinity and inhomogeneous size distribution. In chemical vapor condensation, solid nanostructures or thin films are deposited on a solid substrate from the reaction of vapor phase metal halide or organometallic precursors at high temperatures to synthesize compounds such as FeSi, CoSi, and MnSi, as well as their alloys (including cubic FeGe nanowires[72] and $Fe_{1-x}Co_xSi$ nanowires[73]). During this process, high-purity gas like argon or helium is used in a heated bubbling device comprising the liquid

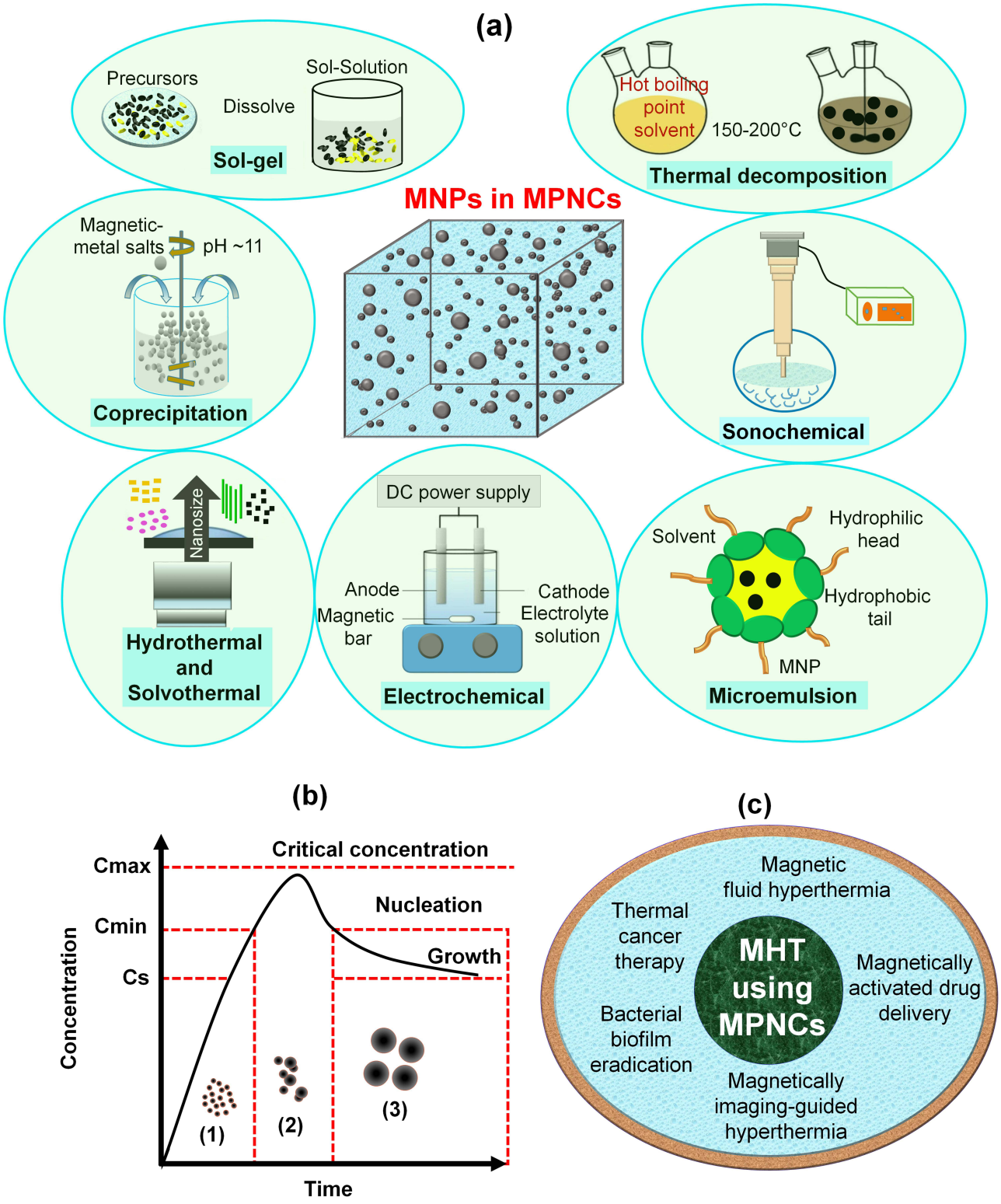

Figure 1 (**a**) Schematic of popular methods for synthesis of MNPs, (**b**) Representation of the principle of nanoparticle nucleation due to LaMer's mechanism of (sulfur) nucleation.[67,68] (**c**) MHT using MNCs for different biomedical applications.[70]

magnetic precursor. Then, it is vaporized at high temperature for producing a flow of carrier gas to deliver the precursor vapor from the heated tubular furnace to the chamber and finally a collection of the magnetic particles. In an innovative study by Farhanian et al,[74] photo-initiated chemical vapor deposition was assisted with a jet-assisted fluidized bed

configuration for a large-scale synthesis of IONPs. In a different technique, sol–gel reactions of condensation and hydrolysis of magnetic salts were used for the synthesis of MNPs.[75,76] Similar to the sol–gel method but with a different hydrolysis reaction, polyol can be used as a reducing and stabilizer solvent to fabricate less aggregated MNPs.[77,78] Polyol approach is commonly applied for enhancing MNPs solubility.[77] In an electrochemical technique (such as laser pyrolysis), localized heating of gas mixture by a continuous wave of CO_2 laser controls the chemical reaction.[79] Table 2 summarizes various fabrication methods and physicochemical properties of MNPs.

Biosynthesis Methods

Bio or green methods are fascinating to improve the biocompatibility of MNPs due to the usage of natural stabilizers and reducing agents such as microbial enzymes and plant extracts with anticancer compounds.[102] In a study by Kumeria et al,[86] green fabrication of superparamagnetic iron oxide nanoparticles (SIONPs) were carried out by using bacteria *mariprofundus ferrooxydans* as a reducing agent. In a different study,[87] a 15 nm spherical-shaped Fe_3O_4 was prepared by a combination of co-precipitation and green synthesis using the reducing agent of bacterial metabolites. It is also worth mentioning that several studies have used plant-based stabilizer/capping agents in the green synthesis methods of MNPs.[103–106]

Physical Methods

The physical method of pulsed wire discharge uses electrical wire explosion in a vacuum, where joule heating vaporizes solid wire to obtain a high-density current over the wire, that subsequently, a shockwave moves out the generated vapor and drops, then it gradually is cooled down at the ambient condition to finally collect the solid MNPs.[107] This technique has various benefits such as a high rate of fabrication, good efficiency of energy transformation, and a reasonable cost of the required devices. As a relatively

Table 2 Various Methods for Synthesis of MNPs

Routes	Methods	Condition	Temp (°C)	Duration (min/hrs/d)	Nano-Size	Capability of Morphology Control	Production Scale	Refs
Chemical	Co-precipitation	Facile in ambient conditions	20–150	Quick (min)	Small	Poor	Large	[80,81]
Chemical	Sol-gel synthesis	Difficult	25–200	Average (hrs)	Small	Good	Normal	[82,83]
Chemical	Electrochemical	Difficult	Room	Slow (hrs - d)	Small	Good	Normal	[84,85]
Green	Biosynthesis	Difficult	Room	Slow (hrs)	Average	Poor	Large	[86,87]
Green	Green-based	Easy	Room	Quick (min - hrs)	Small	Poor	Large	[20,37]
Physical	High-temperature thermal decomposition	Difficult	100–350	Slow (hrs - d)	Very small	Good	Large	[88,89]
Physical	Hydrothermal or solvothermal synthesis	Facile, High pressure	150–220	Slow (hrs - d)	Very small	Great	Large	[90,91]
Physical	Pulsed laser ablation pyrolysis	Difficult	Room	Quick (min - hrs)	Small	Good	Large	[92,93]
Physical	Microwave-assisted	Difficult	Room	Slow (hrs)	Average	Good	Normal	[94,95]
Physical	Microemulsion	Difficult	20–80	Average (hrs)	Small	Good	Small	[96,97]
Physical	Sonolysis or sonochemical	Very facile	20–50	Very quick (min)	Small	Poor	Normal	[98,99]
Physical	Aerosol/vapor	Difficult, controlled conditions	Above 100	Average (min- hrs)	Small	Good	Large	[100,101]

simple and recent method, microwave-assisted procedure uses the magnetic precursors' mixture under the external electric field of the microwave for triggering molecule reorientation and homogeneous inner heating reactions to synthesize MNPs. The thermal decomposition technique has been recommended based on two classifications: i) conventional reaction method with primary processes at room temperature and subsequently at high temperature in an open or closed reaction vessel and ii) hot-injection method as precursors were injected into the heated reaction mixture. MNPs with desired physicochemical properties are also fabricated through low-cost hydrothermal methods using organic solvent instead of water in the reaction medium. For instance, Fe_3O_4 NPs were successfully fabricated using a mixture of Fe salts, urea, sodium citrate, and acetate in ethylene glycol solution to obtain a homogeneous dispersion as the reaction mixture was then transferred to an autoclave and heated up to 200 °C for 24-hr.[88] Another interesting procedure for MNPs fabrication is microemulsion, where the surfactant molecules are presented at the interface border area of oil and water via a monolayer, which can be based on oil/water (oil dispersed in water) or water/oil (water dispersed in oil). In this particular case, the surfactant molecules with hydrophobic and hydrophilic tails and head, respectively, are dissolved within the oil and water phase or inversely.[108] In this method, the most common surfactants are polyvinyl pyrrolidone (PVP), cetyltrimethylammonium bromide, sodium dodecyl sulfate, and bis (2-ethylhexyl) sulfosuccinate. MNPs with a complex design have been fabricated by sonolysis or sonochemical methods using high acoustic waves and cavities or bubbles to generate 5000 °C and 1800 kP pressure in a short reaction time.[98] In addition to the above-mentioned procedures, MNPs can be fabricated through flow injection (with high reproducibility) and aerosol/vapor technique.

Investigating the Toxicity of Magnetic Nanomaterials

Toxicity issues are vital aspects of the drug delivery systems and cancer therapy. The toxicity of MNPs can be relevant to various parameters, including dose-dependency, duration, concentration, and physicochemical characteristics (such as surface modification, dimension, and shape) of MNPs.[109] García et al investigated the in vitro toxicity of copper, titanium dioxide, $CuZnFe_2O_4$, and IONPs at concentrations ranging between 20 and 100 μg/mL and found no toxicity from the tested IONPs.[110] Despite this, the surface of bare MNPs may exert toxicity associated with their large surface area and the generated reactive oxygen species (ROS), due to the inadequate reduction of oxygen. ROS can be produced via the leaching of metal ions, or release of oxidants via enzymatic degradation of MNPs.[111] The inflammatory response of cells with an increased amount of ROS triggers oxidative stress and subsequently attacks the cellular proteins, lipids, and DNA, causing carcinogenesis, necrosis, apoptosis, and finally cell death.[112] This reflects that the amount of administered MNPs must be precisely controlled. After the administration of MNPs, the ratio of ROS generation can be analyzed via dichlorofluorescein diacetate as a fluorescent marker. It is worth mentioning that ROS may also eliminate damaging cancer, for instant.[113] In a report,[114] 25 μg/mL spherical Fe_3O_4 MNPs (72.6±0.6 nm) showed damages against erythrocytes for in vitro study to analyze the eryptosis indices. For the in vivo evaluation using female CD® IGS Rats at 8 weeks of age, 12 mg/kg Fe_3O_4 NPs caused apoptosis of circulating erythrocytes. In short, Fe_3O_4 NPs caused pathological changes in cell membranes, and oxidative stress caused cancer cell elimination in vitro and also in vivo.[114] In order to decrease the toxicity against normal cells, MNPs have been incorporated with various counterparts and coating agents to synthesize MNCs and PMNCs with increased multifunctional properties, biocompatibility, and free magnetic ions onto the target organ causing oxidative stress and toxicity against target cancer cells. In a study, bare MNPs and n-octyltriethoxysilane-coated MNPs were fabricated for anticancer analysis using ReNcell VM (human neural stem cells) and PC12 (rat pheochromocytoma) at different concentrations from of 0–64 μL for 24 h.[115] The results showed the higher safety and biocompatibility from coated MNPs than uncoted MNPs. In a different study,[116] bare nanomagnetite, starch-coated nanomagnetite, and dextran-coated nanomagnetite were utilized in toxicity assays on rat pheochromocytoma PC12 tumors at a concentration range of 0.01–0.5 mg/mL for 1, 2, 3, 24, 48 and 72-hr. In the XTT cytotoxicity assay, bare nanomagnetite was on the outer surface and unable to enter the cells without any killing effects up to 0.1 mg/mL; however, 49% cell death was indicated at 0.25 mg/mL after 72-hr. Starch-coated nanomagnetite had insignificant cell death during 24-hr, whereas it caused 30% cell death at 0.1 mg/mL after 72-hr. In addition, at 0.25 mg/mL, it indicated almost 100% killing effects against PC12 tumors after 72-hr. The anticancer effects of dextran-coated nanomagnetite were ineffective at concentrations up to 0.1 mg/mL; however, it was significantly enhanced at 0.25 mg/mL after 72-hr and also 24-hr. Overall, this study aimed to indicate the positive influence of coating for MNPs and also the effects of incubation time and concentration of MNPs in the elimination of PC12 cells. It is worth to mention that the pharmacokinetics and degradation pathway of counterparts of MNCs such as MNPs cores and polymer coating agents could be the potential limitations for the clinical usage of innovative MNCs.[117]

The specific dosage of the magnetic complex to eliminate 50% of the tested animals in a required duration can be measured by LD-50.[118] In an interesting study, LD-50 of dextran-coated IONPs (2000–6000 mgFe/kg) was almost ten times higher than that of uncoated IONPs (300–600 mgFe/kg body).[119] Similarly, IONPs coated with carboxy-dextran revealed the LD-50 value of 35 mmol Fe/kg,[120] showing the positive effects of coating MNPs in the body's innate biological response related to an appropriate dose of the administered MNPs.[118] In vivo study indicated that almost 100% dextran-coated IONPs were cleared from the blood of rats 84 days post-injection.[121] It should be mentioned that there is still insufficient evidences to understand the degradation and extended circulation time of magnetic materials in the body, since it requires long-duration monitoring for in vivo toxicity (months or even years), and also ethical issues of immolating numerous animals for LD-50 analysis. In addition, FDA does not consider the customary LD-50 analysis anymore. As an alternative procedure, in vitro analysis was suggested; however, it caused low number of metabolic actions of cell lines with less required regulatory parameters for various types of cells. In the future toxicity studies, it is therefore vital to evaluate further toxicity evaluations of MNCs in the human body.

Application of Polymer in Stabilizing Magnetic Nanocomposites

Polymer-based nanocomposites with pH-responsive structures could be promising nanodrug systems for future cancer treatment.[122,123] However, changing pH in the human body is a long time process with incapability to be adjusted externally. This issue can be tackled via using polymers as solid supports or coating agents for MNPs as fillers to fabricate multifunctional polymer-based magnetic nanocarriers as remotely controlled drug delivery systems.[124,125] Biopolymer is the most abundant polymer on earth with low cost, desired biocompatibility, biodegradability, and physicochemical properties.[126] It should be considered that some synthetic and also natural polymers have issues of instability, low biocompatibility, undesired biodegradability, and high-cost chemical modifications.[12] As natural excipients, various polysaccharides such as chitosan, alginate, dextran, nanocellulose, pectin, hyaluronic acid, starch, pullulan, guar gum, glycogen, beta mannan and inulin can be used in advanced anticancer nano-drug systems.[12] Table 3 shows some polysaccharides utilized in the fabrication of biocomposites. Only two polysaccharides of chitosan and curdlan are cationic, while other listed polysaccharides are anionic or neutral. Polysaccharides can

Table 3 Various Polysaccharides Utilized in Composites

Polysaccharide	Source	Charge	Main Functional Groups	Ref.
Cellulose	Botanical and bacteria	Negative	OH	[138]
Chitosan	Shells of crustaceans such as shrimp, lobster, crayfish and oyster	Positive	OH, COO^{-}, NH_2	[9]
Starch	Microbial product in wine, glucose, plants	Neutral	OH	[139]
Alginate	The cell wall of brown marine algae	Negative	OH, COO^{-}	[140]
Mannan	Plant	Neutral	OH	[141]
Hyaluronic acid	Connective, epithelial, and neural tissues	Negative	OH COOH	[142]
Heparin	Animal tissues	Negative	OH OSO_3H	[143]
Pullulan	Fungus *Aureobasidium* pullulans	Neutral	OH	[144]
Levan	Archaea, fungi, bacteria, and a limited number of plant specie	Neutral	OH	[145]
Elsinan	Fungi, bacteria	Neutral	OH	[146]
Gellan	Bacterium Sphingomonas elodea	Negative	OH	[147]
Curdlan	Fungi, bacteria	Positive	OH, COO^{-}	[148]
Succinoglycan	Agrobacterium sps, Rhizobium sps, Rhizobium meliloti, Alcaligenes faecalis	Negative	OH	[149]
Zooglan	Zoogloea ramigera	Negative	OH	[150]
Xanthan	Xanthomonas campestris	Negative	OH	[151]
Dextran	Leuconostoc mesenteroides, Lactobacillus spp and Streptococcus mutans	Neutral	OH	[152]

be obtained from different plants, vegetables, fruits, grains, glycogen, and red alga (such as Glaucocystis, and Chaetomorpha melagonicum), liver and muscles of animals such as ascidians, and some bacteria.[127,128] In polysaccharides, glycosidic linkages bound many monosaccharides with long chains. In drug delivery applications, natural cellulose and chitosan are the first and second most popular polysaccharides, respectively. The polysaccharide-based products possess desirable properties, including the capability to bind with various drugs, great swelling behavior, pH gradient behavior, and high biodegradability for innovative antitumor drug delivery systems.[129] Each property has its particular pros and cons for developing a topical nanodrug formulation with improved stability and therapeutic effects.[130] The vitality of drug-loaded polysaccharides and polymers is a consequence of their potential to deliver a desirable amount of drugs to cancer cells without significant effects against normal cells.[130,131] For example, curcumin was loaded onto crystalline nanocellulose and caused almost three times higher colorectal cancer cell death than that of curcumin alone.[132] The side-effects of chemotherapy have been alleviated by loading a sufficient dosage of chemo-drugs onto various polymer-based carrier systems, for instance, poly(2-vinyl pyridine)-b-poly(ethylene oxide) nanomicelles,[133] chitosan microspheres,[134,135] carboxymethyl cellulose,[136] and crystalline nanocellulose to name a few.[137] Thus, with the immense demand for using biocompatible nanocarriers in anticancer drug delivery systems, natural polysaccharides should be explored for advanced cancer treatments.

In MNCs, various coating materials and surface functionalization with peptides, antibodies, small molecules, and aptamers could improve the colloidal stability, functionalities, and other advantages of MNPs for biological regimes and magnetothermal chemotherapy to obtain combination therapy of MHT and magnetic targeting, switchable synthetic cell surfaces, and magnetothermal chemotherapy. The most well-known coating for MNPs are organic materials (like surfactants, polymers, and biological molecules), and inorganic materials (such as metals and metal oxides) (Figure 2). The popular biocompatible polymers used in MNCs are dextran, PVP, starch, albumin, polyethylene glycol (PEG), chitosan, ethylcellulose, polyethylenimine (PEI), polymethyl methacrylate (PMMA), polyacrylic acid (PAA), polylactic acid (PLA), polyvinyl alcohol (PVA), citric acid, glucuronic acid, gelatin lipids, liposomes, dendrimers, polyacrylamide, and bisphosphonates. Various studies have reported the fabrication of different MNCs (with various size ranges) by using chitosan-coated $MnFe_2O_4$ (18 nm),[153] dextran-coated Fe_3O_4 (21 nm),[154] cellulose matrix (87.12 nm)/Fe_3O_4 fillers (11.01 nm),[80] PEG-coated $NiFe_2O_4$ (16 nm),[155] phosphate-coated Fe_3O_4 (14 nm),[156] tetraethyl orthosilicate coated $MnFe_2O_4$ (14 nm),[157] $Zn_{0.9}Fe_{0.1}Fe_2O_4$ (11 nm),[158] stevioside-coated Fe_3O_4 (3 nm),[159] citric acid-coated $Mn_xFe_{3-x}O_4$ (34 nm),[160] aminosilane-coated Fe_3O_4 (100 nm),[161] and oleic acid-coated Fe_3O_4 (45 nm).[162]

MNCs have various shapes and structures, including core-shell, shell-core, matrix dispersed, shell-core-shell, yolk, dumbbell, and Janus (Figure 3).[164,165] In core-shell, either organic or inorganic materials coat the magnetic core.[166,167] However, if the magnetic core is not centered, it is called "yolk" form.[168] When the magnetic core is placed between two functional materials, it is termed shell-core-shell NPs. In a matrix dispersed system, a matrix acts as the dispersant agent for MNPs to avoid aggregation over large clusters and possibly maintain superparamagnetism. Janus NPs are associated with two sides of a magnetic core and different functional materials.[169,170]

In a study by Wulandari et al,[172] Fe_3O_4 NPs were fabricated by the ex-situ co-precipitation method and cross-linked with chitosan using tripolyphosphate/sulfate. The results from scanning electron microscopy (SEM) and X-ray diffraction (XRD) spectrum revealed that the increase of chitosan coating agent enhanced and declined the SEM size and crystallite size of the NPs, respectively. In different investigations, the in-situ fabrication of MNPs was reported via dispersing the iron ions in the polymer particles for subsequent MNP nucleation as conjugated strongly with functional groups of the polymer to synthesize PMNCs.[50,173,174] Recently, Malhotra et al[175] synthesized bare Fe_3O_4 NPs through co-precipitation method followed by the use of hydrothermal method at 200 °C and carbonized organic starch (0.19 g) to simultaneously functionalize and also coat the bare Fe_3O_4 (0.5 g) abbreviated as Fe_3O_4@C (Figure 4a–g). Compared to the bare MNPs, the transmission electron microscope (TEM) image of Fe_3O_4@C exhibited better dispersion and bigger sizes ranging from 16 to 52 nm with around 2 nm thickness of the carbon coating. Raman spectrum of both Fe_3O_4 and Fe_3O_4@C displayed peaks at 660–680 nm attributed to the presence of MNPs, whereas Fe_3O_4@C showed additional peaks between 1100 and 1800 cm^{-1} related to the formation of diamond-like carbon (Figure 4C). Fe_3O_4 and Fe_3O_4@C exhibited analogous XRD results (Figure 4D) with an average crystallite size of 18 nm and 24 nm, respectively, since the hydrothermal process did not damage the crystalline structure of Fe_3O_4@C. From Figure 4E,

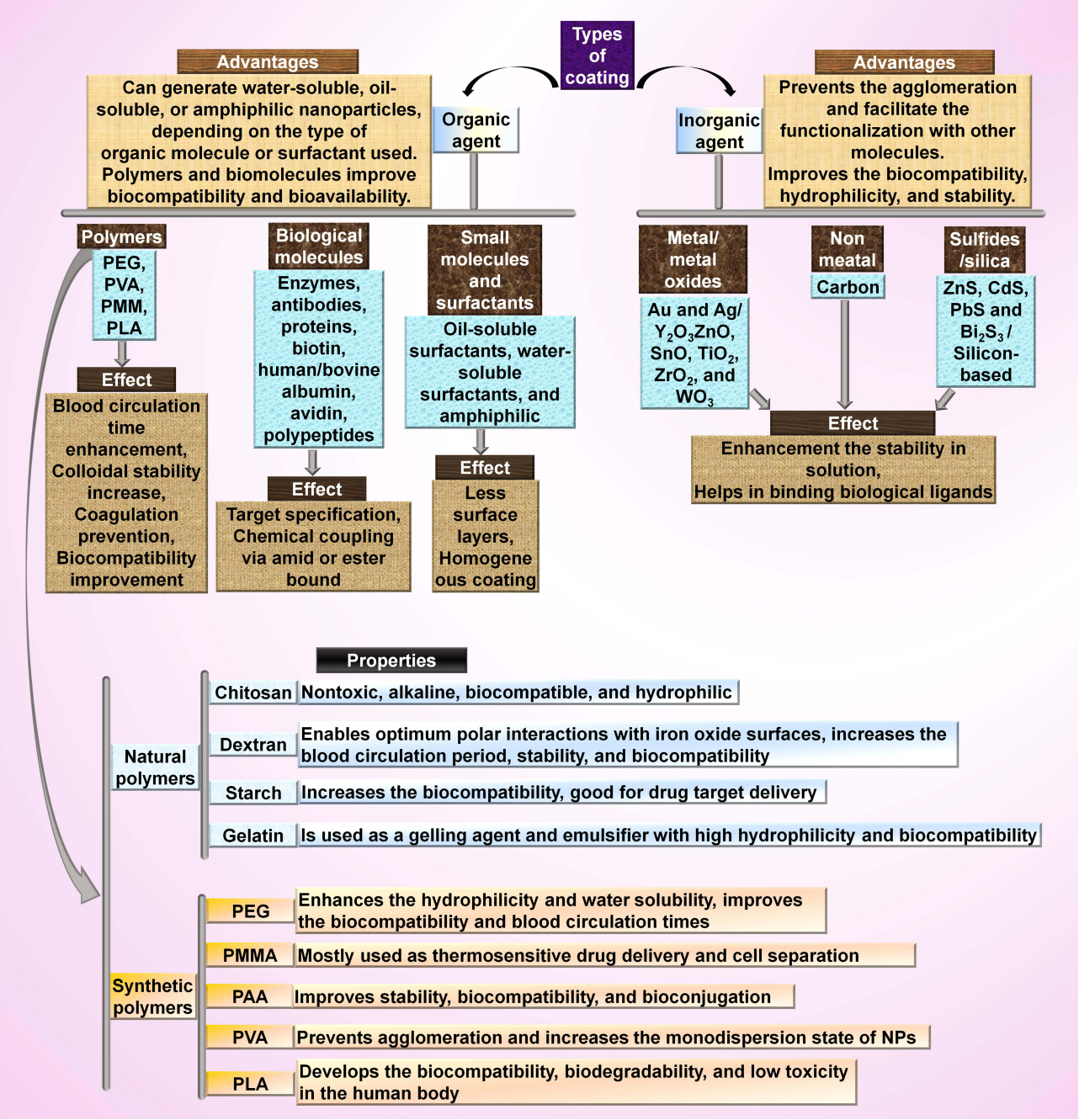

Figure 2 Inorganic and organic materials and their properties regarding their use as functionalizing and coating agents for the synthesis of MNCs.[163]

Fourier-transform infrared spectroscopy (FTIR) spectrum of the samples indicated the magnetite formation with the peaks at 572 cm^{-1} and 700 cm^{-1}. Thermogravimetric analysis (TGA) for Fe_3O_4 and Fe_3O_4@C displayed a weight loss of ~2.6% and ~0.4% at 40 °C−115 °C, respectively. Interestingly, the saturation magnetization (M_s) of Fe_3O_4@C (135 emu/g) was higher than Fe_3O_4 (94 emu/g) (Figure 4G); thus, the coated Fe_3O_4 NPs revealed better multifunctionality and physicochemical properties than the uncoated Fe_3O_4 NPs. Furthermore, from the results of cytotoxicity assays using model organisms of adult zebrafish, Fe_3O_4@C was safer and less toxic than uncoated Fe_3O_4. The above examples indicate the positive effects of polymer coating for MNPs to fabricate PMNCs with high colloidal stability, desired size ranges, improved functional groups, and biocompatibility.

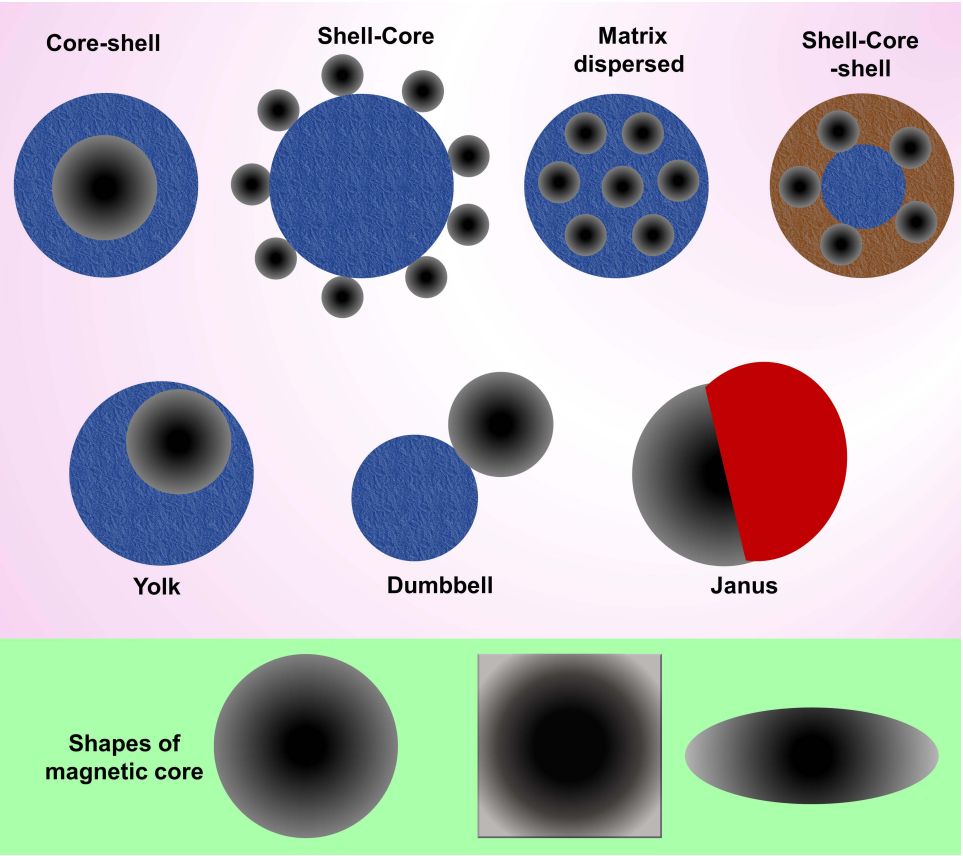

Figure 3 Different coating structures for synthesis of MNCs and common shapes of the magnetic core.[171]

Studying the Methods Used in the Hyperthermia and Cancer Treatment Based on Magnetic Nanocomposites

In advanced drug delivery systems, MNCs can show controlled and precise release of drug under adjustable conditions, including electric and magnetic fields, ultrasound waves, heat, light, enzymes, and pH changes.[45] MHT (known as magnetic thermal ablation or magnetic thermotherapy) has been a distinctive technique in cancer treatment for nearly past five decades with the vitality related to using a noncontact, safe, and low-cost external heating source of AMF (typically 50–1000 kHz). In this treatment method, the temperature is commonly ranged from 42 °C to 48 °C onto accumulated MNPs at the target malignant tissue to effectively kill cancer cells with negligible or no damage against healthy cells.[44] MHT can use various drug-loaded MNCs to i) closely control the heating yield by adjusting the applied AMF, ii) maintain the efficiency of the cancer treatments without detrimental side effects, and iii) consumption of less drug-administered to overcome the treatment shaping problems in the conventional chemotherapy alone.[17,176] Moreover, AMF is potentially capable of achieving "on/off" drug release from MNCs in target tissue with treatment scale-up capability compared to chemotherapy and surgery, which are confined to poor cancer treatment index and harmful side effects. The AMF strengths regulate hyperthermia temperature in the cell medium through the heating capacity of a magnetic nano heater measured by specific absorption rate (SAR) or the specific loss power (SLP).[37,177] Figure 5a shows the schematic magnetic hyperthermia procedure and thermal dissipation procedure, including Néel and Brownian relaxation processes from MNCs under AMF. The increased temperature positively increases physical rotation of magnetic particles, which subsequently can improve M_s, magnetic anisotropic constant (K), and a Brownian heating loss mechanism.[44,178,179] In this manner, the SAR value of MNPs is related to M_s (Figure 5bi), whereas the highest SAR value is at a K (Figure 5bii) and specific NPs size (Figure 5biii) for obtaining enhanced biological effects. Furthermore, the SAR value is attributed to morphology, composition, and concentration of MNPs, as well as the amount of the

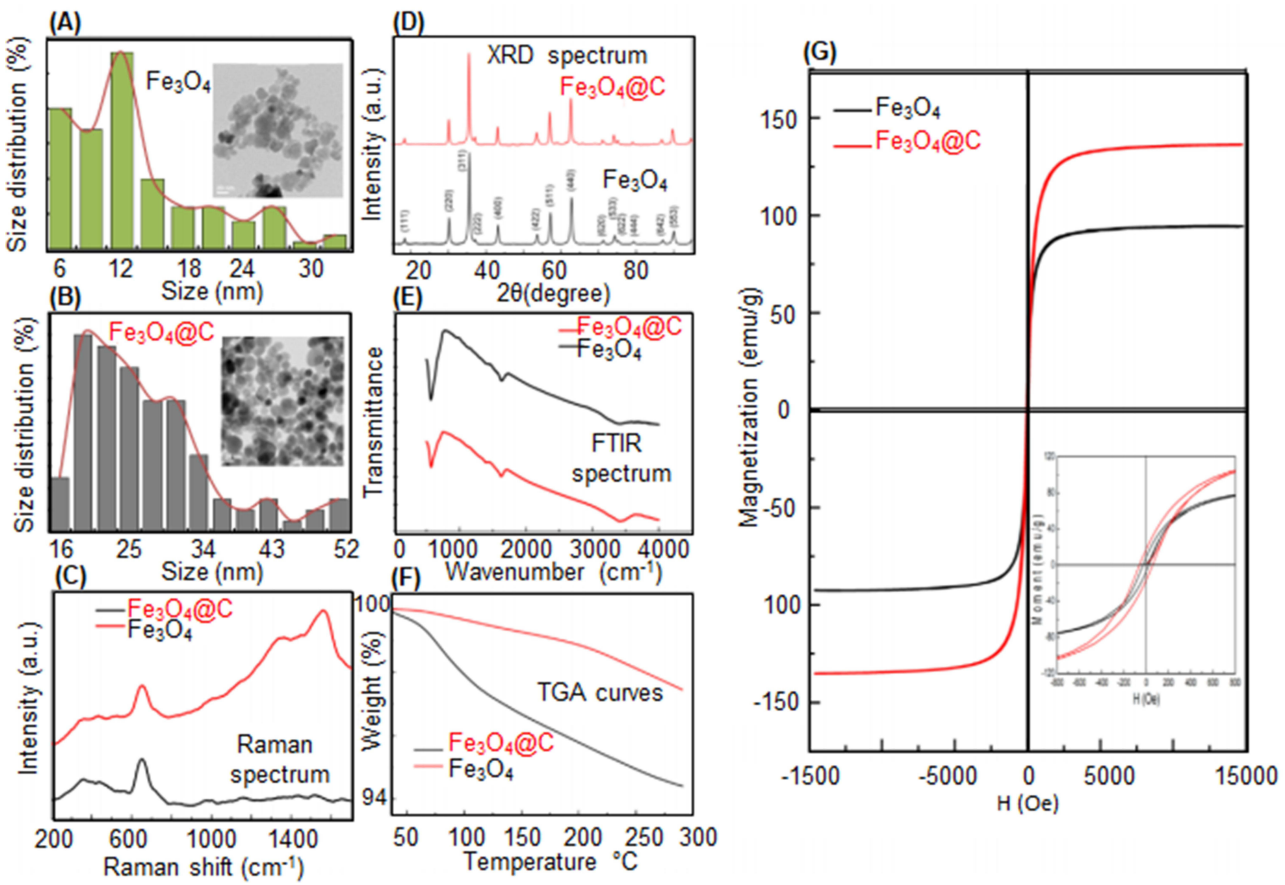

Figure 4 TEM morphologies and size distribution of (**A**) Fe_3O_4 NPs and (**B**) PMNCs of Fe_3O_4@C. (**C**) Raman spectrum, (**D**) XRD, (**E**) FTIR spectrum (**F**), TGA curves, and (**G**) M_s of Fe_3O_4 and Fe_3O_4@C.[136]

generated heat by a unitary ratio of magnetic particles per time under the exposure of AMF.[19,180] As schematically shown in Figure 5a, during the hyperthermia process, magnetic nanofluids are placed in the middle of a helical coil with several turned-loops connected to a water-cooled system. Also, currents of AMF introduce different frequencies and field strengths in order to increase the temperature for paramount effects of MHT. For the precise measurement of SAR value, the dT/dt graph is obtained from the initial slope of the temperature and time curves using the linear fitting method classified into the initial slope, full-curve fit method, and corrected slope. The initial slope method relies on the initial temperature changes without measuring the complete heating curve as a non-linear temperature rises to underestimate SAR values by 25%. The full-curve fit technique is able to estimate 10% accuracy for the SAR value. The third and most accurate technique is the corrected slope. More details on several proposed methods to calculate SAR from heating data are explained well in different studies.[181,182] The SAR values of several MNPs and MNCs are listed in Table 4. In a recent study, the applied AMF increased the temperature of MNPs (13 nm) up to 42 °C after 128 sec with the SAR value of 350 W/g.[183] This study concluded that the fabricated MNPs with a TEM size of around 10 nm is appropriate for the hyperthermia test, while it did not consider that enhanced temperature of MNPs within the secure hyperthermia range (42–48 °C) is appropriate for MHT. It should be noted that different studies stated that the secure hyperthermia range can be in the range from ~42 °C to ~48 °C.[20,37,44,184,185] The generated temperature from AMF ranging from 42 to 48 °C causes the cells to favorably undergo apoptosis, however above this range, they mostly undergo necrosis,[186,187] in which the cell elimination by apoptosis is preferable over necrosis to prevent unwanted inflammation and metastasis.[187] Furthermore, above 50 °C and 200 °C may eventuate in coagulation and undesired burn at the affected areas.

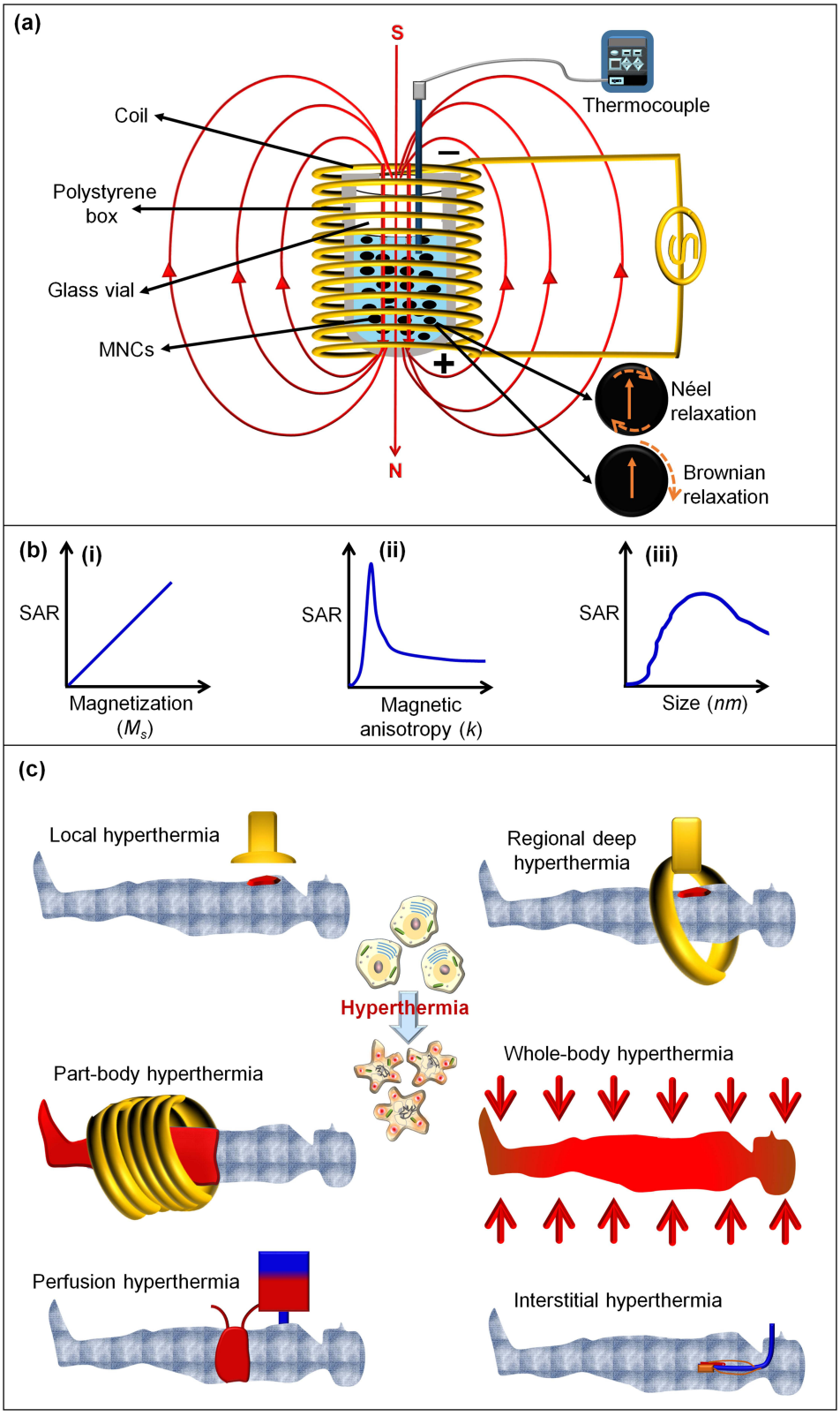

Figure 5 (**a**) Schematic presentation of thermal dissipation process (Néel and Brownian relaxation processes) from MNCs under AMF.[188,189] (**b**) The SAR value of MNPs related to (i) M_s, (ii) K, and (iii) particle size (r) with SLP, respectively.[188,189] (**c**) Illustration of different methods for hyperthermia treatment.[190]

Table 4 Overview of the Recent Studies on SAR Values of MNPs, MNCs, and PMNCs with Respect to Size, Morphology, and Factors Used in Magnetic Hyperthermia Analysis

Magnetic Composites	Type of Analysis, Shape, Size (nm)	Field (kA/m)	Frequency (kHz)	SAR (W/g)	Ref.
Fe_3O_4/poly(styrene-co-maleic anhydride)	TEM, nanoclusters, 33	23.8	302	253	[191]
Fe_3O_4/PVP	TEM, spherical, 45	32.5	400	1100	[192]
Fe_3O_4/graphene oxide	TEM, spherical, 45	32.5	400	5160	[192]
$CoFe_2O_4$	TEM, spherical, ~ 10	30.1	265	91.84	[193]
Ag-Fe_3O_4	TEM, spherical, ~ 10	13.9	274	43	[194]
$NiFe_2O_4$	TEM, spherical, 4.4	23.7	170	~ 11	[195]
Fe_3O_4/PEG	TEM, cubes, 19	29	520	2452	[196]
$CoFe_2O_4$	TEM, spherical, 5.4	95.6	329	~76	[197]
$Co_{0.03}Mn_{0.28}Fe_{2.7}O_4/SiO_2$	TEM, spherical, ~22	33	380	~3417	[198]
Fe_3O_4/citric acid	TEM, spherical, ~10	35.88	316	49	[199]
Fe_3O_4/PEG	TEM, spherical, ~10	35.88	316	56	[199]
Fe_3O_4/ethylene diamine	TEM, spherical, ~10	35.88	316	77	[199]
Fe_3O_4/cetyl-trimethyl ammonium bromide	TEM, Spherical, ~10	35.88	316	47	[199]
Fe_3O_4/citric acid/PEG	TEM, spherical, ~10	35.88	316	60	[199]
$Zn_{0.5}Ca_{0.5}Fe_2O_4$	TEM, spherical, 12–14	10.2	354	~14.8	[200]
$Zn_{0.33}Fe_{2.67}O_4$	TEM, spherical, ~8	35.7	360	~178	[201]
Gd-doped Mg-Zn ferrites	TEM, spherical, 50–200	5.0	600	~15–27.5	[202]
Fe_3O_4/garcinia mangostana fruit peel extract	TEM, spherical, ~13	75	318	98	[20]
		100	313	130	
		125	312	179	
Fe_3O_4/*Punica Granatum* fruit peel extract	TEM, spherical, ~11	75	318	196	[203]
		100	313	212	
		125	312	232	
Fe_3O_4	Nr	0.450	400	46.8	[204]
Fe_3O_4@agar	TEM, spherical, 9.2	0.450	400	23.6	[204]
Chitosan/trimethylammonium/ SPION	TEM, spherical, 13.7	27.57	360	168	[205]
Chitosan/curcumin/alginate/SPION	Nr	27.57	360	280	[205]
Peptide nucleic acid oligomers/SPION	TEM, spherical, ~15	17	183	65	[206]
$CoFe_2O_4$/meso-2,3-dimercaptosuccinic acid/DOX	TEM, spherical, 13	30	307	94.58	[207]
Chitosan/Fe_3O_4/5FU	SEM, spherical, 125	35	180	Nr	[208]
$Fe_{3-\delta}O_4$@silane and a thermoresponsive copolymer shell composed of 2-(2-methoxy)ethyl methacrylate and oligo (ethylene glycol)methacrylate moieties (1.14 mL)	TEM, spherical, 10	23.8	536.5	25.2	[209]

(*Continued*)

Table 4 (Continued).

Magnetic Composites	Type of Analysis, Shape, Size (nm)	Field (kA/m)	Frequency (kHz)	SAR (W/g)	Ref.
$Fe_{3-\delta}O_4$@silane and a thermoresponsive copolymer shell composed of 2-(2-methoxy)ethyl methacrylate and oligo (ethylene glycol)methacrylate moieties	Dynamic light scattering (DLS), Not reported (Nr), 55–80	23.8	536.5	61.7	[209]
$Fe_{3-\delta}O_4$@silane	DLS, Nr, 20–30	23.8	536.5	100	[209]
Graphene quantum dots-Fe_3O_4/SiO_2	TEM, Nr, 100	14.3	409	44	[210]
DOX loaded Fe_3O_4/MamC/proteinAR-3 mAbs (IgG1)	TEM, Nr, 36	12.5	273	53	[211]
			205	41	
			163	22	
			143	19	
Magnetite	TEM, spherical, 30	12.5	273	68	[211]
			205	47	
			163	28	
			143	24	
Alginate-chitosan-Fe_3O_4	Nr	40	265	720	[212]
$CuFe_2O_4$	TEM, spherical, 17.3	28.5	126	192	[213]
		25.7	126	185.2	
		22.2	126	177.8	
		18.6	126	171.5	
$CuFe_2O_4$	TEM, spherical, ~19.9	19	120	44.9	[91]
		16	120	38.0	
		13	120	24.8	
$CuFe_2O_4$	TEM, spherical, ~25	13.5	331	6.48	[95]
$Mn_{0.5}Zn_{0.5}Fe_2O_4$	TEM, spherical, ~14	6.37	178	28.38	[214]
$MgFe_2O_4$	TEM, spherical, ~9	9.2	198	~19	[215]
Solvent optimized redox tuned iron oxide	TEM, spherical, ~25	50	100	~700	[216]
Thermosensitive polymer poly(2-(dimethylamino)ethyl methacrylate) coated Fe_3O_4	SEM, irregular–quasi-spherical, 98	16.15	205	150	[217]
Fe_3O_4/hexadecylamine/oleic acid/1-octanol	TEM, rods, ~56 (length) × 10 (width)	63.81	310	862	[218]
Graphene oxide-Fe_3O_4-PEG	TEM, spherical, ~20	12.57	293	557.38	[219]
PLGA/Fe_3O_4/DOX/PVA	TEM, spherical, 172	2	205	36.27	[220]
PLGA/Fe_3O_4	Nr	2	205	35.73	[220]
Cetyltrimethylammonium bromide@Fe_3O_4	TEM, cubic, ~ 80	63.66	315	1036	[221]

(*Continued*)

Table 4 (Continued).

Magnetic Composites	Type of Analysis, Shape, Size (nm)	Field (kA/m)	Frequency (kHz)	SAR (W/g)	Ref.
Fe_3O_4	TEM, Pseudo spherical, 12.97	15.9	252	63.4	[222]
Fe_3O_4@citric acid	DLS, 46.9	15.9	252	65.8	[222]
Fe_3O_4@(3-aminopropyl)triethoxysilane	DLS, 68.1	15.9	252	67.2	[222]
Fe_3O_4@dextran	DLS, 76.6	15.9	252	55.6	[222]
SPIONs coated with $PEG_{4.9kD}$-$PLA_{6.0kD}$	TEM, Cubic, 18	59.6	346	558	[223]
IONPs	TEM, Cubic, 30–35	63.3	310	800	[224]
Chitosan coated Fe_3O_4	TEM, spherical, 37	14	335	595	[84]
Fe_3O_4	TEM, cubic, 37	23.9	571	213	[98]
$mSiO_2$@Fe_3O_4	TEM, spherical, ~100	22	120	13.84	[89]
Poly(Nisopropyl acrylamide-co-acrylic acid)@$mSiO_2$@Fe_3O_4	TEM, spherical, ~100	22	120	8.22	[89]
Fluorescent IONPs/PLGA conjugated with human epidermal growth factor receptor 2	DLS, Nr, 524	16.27	440	183	[225]
IONPs - (poly(maleic anhydride-alt-1-octadecene)-(tetramethylrhodamine 5(6)-carboxamide cadaverine - N-(3 dimethylaminopropyl)-N′-ethylcarbodiimide hydrochloride - 4-aminophenyl β-D glucopyranoside	TEM, spherical, 11.3	20	829	104	[226]
PEG coated SPIONs	TEM, spherical versus cubic, 33	9.35	300	1010	[227]
PEG coated SPIONs	TEM, spherical versus cubic, 40	20.7	300	1026	[227]
Chitosan coated Fe_3O_4	TEM, spherical, 30–40	20	335	711	[228]
Graphene oxide-Fe_3O_4	TEM, spherical, 10–21	16.72	325	543	[85]
Silica coated lanthanum strontium manganese oxide	TEM, irregular, 35	13	335	295	[229]
Chitosan-g-N-isopropylacrylamide coated Fe_3O_4-silica	TEM, spherical, 30–50	3	100	9.75	[230]
Fe_3O_4	TEM, spherical, 5–10	3	100	15.80	[230]
Trimesic acid coated SPIONs dispersed in triethylene glycol	TEM, spherical, 9	10.9	751.5	276.3	[231]
		13.8	262.2	81.2	
Tetraethyl orthosilicate coated $La_{0.7}Sr_{0.3}MnO_3$	TEM, wormhole-like mesopores, 45	14	350	255	[232]
Citric acid coated $Ho_xFe_{3-x}O_4$	TEM, spherical, 10–15	23.87	488	337.3	[233]
Pluronic F127 coated $Mn_{0.6}Ga_{0.4}Fe_2O_4$	Nr	10.18	354	160.9	[234]
Cetyltrimethylammonium bromide and polycaprolactone coated Fe_3O_4	TEM, spherical, 21	15.75	312	255.12	[235]
Aminosilane coated Fe_3O_4	DLS, Nr, 100	23.87	557	320	[161]
Dextran coated Fe_3O_4	TEM, irregular, 21	11.93	150	52.3	[154]

(*Continued*)

Table 4 (Continued).

Magnetic Composites	Type of Analysis, Shape, Size (nm)	Field (kA/m)	Frequency (kHz)	SAR (W/g)	Ref.
Polyphenol coated Fe_3O_4-γFe_2O_3	TEM, spherical, 10–14	23.87	570	Nr	[236]
Fe_3O_4	TEM, spherical, 27	Nr	13,560	725	[237]
Citric acid coated $Mn_xFe_{3-x}O_4$	TEM, spherical, 34	13.36	405	Nr	[160]
Stevioside coated Fe_3O_4	TEM, spherical, 3	13.36	405	80	[159]
Oleic acid coated Fe_3O_4	TEM, Nr, 45	26.67	265	80	[162]
Chitosan coated $MnFe_2O_4$	TEM, cubic, 18	60	307	270	[153]
PEG $NiFe_2O_4$	TEM, rod, 16	3.89–5.49	260	17–22	[155]
Phosphate coated Fe_3O_4	TEM, spherical, 14	0.819	126	11.1	[156]
Tetraethyl orthosilicate coated $MnFe_2O_4$	TEM, spherical, 14	5.49	260	47.8–84.65	[157]
$Zn_{0.9}Fe_{0.1}Fe_2O_4$	TEM, spherical, 11	2.73	700	36	[158]

The Methods of Hyperthermia Therapy

Hyperthermia treatment with noninvasive properties is among procedures that have been exposed to intensive studies for treatments of various tumors with diverse biological regimes and sizes at different parts of the body.[238,239] Even without using a magnetic nano heater, hyperthermia techniques have been used in development of desired heat induction for eliminating tumor tissues with negligible damage to the surrounding normal cells.[185,240] The hyperthermia systems with the capability to regulate the topical heat induction and effectiveness have conferred to be classified into the following methods: local, localized deep, whole-body, part-body, perfusion, and interstitial hyperthermia (Figure 5c).

Investigation of Local and Localized Deep Hyperthermia

External local hyperthermia using heating devices is a coordinated therapy to target small areas of superficial tumors and selectively raise the therapeutic temperature (39–45 °C) of tumor cells under the skin. This method was used for the treatment of laryngeal cancer, neck cancer, and dendritic cell.[241] For example, local hyperthermia decreased 25% of the tumor size located at tongue squamous cell carcinoma; however, it showed the ineptitude of heat dose control and localized treatment for tumors located at supraclavicular, head, and neck areas.[241] Endocavitary and interstitial hyperthermia are subtypes of local hyperthermia to eliminate the superficial tumors via implanting the applicator (with diameter below 5 cm) onto the tumor and provide heat source of radio wave, microwave, or ultrasound using antennas, which can be challenging and uncomfortable for the patients.[239,242] Antennas or applicators release microwaves or radio waves, to increase the temperature on the surface of superficial tumors via a contacting medium.[242] For endocavity hyperthermia, the applicator is placed within the hollow organs including the rectum, urethra, cervix, and vagina, whereas, for interstitial hyperthermia, the applicator is placed within the interstitial area for the treatment of recurrent head and neck, breast, and prostate cancer.[239] Rather than the whole-body treatment, localized deep hyperthermia increases the controlled heat around 42 °C to trigger the desired thermal damage at targeted deep-seated tumor area for the elimination of tumor cells such as peritoneal.[239] In principle, it is normally applied for treatments of diseases in deeper tissues by microwaves radiofrequency, and ultrasound methods.[243]

Study of Whole-Body, Part-Body, and Perfusion Hyperthermia

Whole-body hyperthermia has been used as treatment of many different diseases for several decades.[244] It was traditionally used for fever therapy by covering the patient with plastic sheets, hot liquid, a hot water jacket suit, and a heated bed to increase the blood flow and the whole body temperature up to 40 °C for increasing the permeability of

cancer cell membrane with higher heat sensitivity than normal cells for subsequent treatment of the metastatic tumors.[239] The most popular procedures of whole-body hyperthermia are flexible infrared chambers by heating the patient's room and wrapping them with a warm blanket. The maximum heat of 42 °C for around 1-hr can be appropriate,[245] albeit some systemic issues were reported for heart, blood vessels, and main body organs along with major side effects such as diarrhea, nausea, and vomiting.[239] Interestingly, a combination of chemotherapy and whole-body hyperthermia treated several kinds of cancer, for instance, ovarian cancer was treated by using whole-body hyperthermia (at 41.8 °C) in combination with carboplatin chemotherapy.[246] In the 1960s, new whole-body hyperthermia via using infrared irradiation started.[244] Based on the report by Jia et al[247] in 2010, commercially available medical whole-body hyperthermia devices are ET Space (Energy Technology, Shenzhen, China) and Oncotherm WBH2000 (Oncotherm, Budaörs, Hungary) and also currently available devices are IRATHERM1000 (von Ardenne Institute of Applied Medical Research, Dresden, Germany) and heckel-HT3000 (Hydrosun Medizintechnik, Müllheim, Germany). More details for hyperthermia therapy can be found from recent publications on whole body hyperthermia[244], thermochemotherapy[248], reirradiation and hyperthermia plus chemotherapy[249], hyperthermia in cancer care[250], and microwave hyperthermia[251].

Intraperitoneal perfusion is another type of hyperthermia therapy to treat a metastatic tumor in the abdominal area via using hot liquid to raise the temperature to around 45 °C[239] for treatments of various types of cancer, including colorectal and ovarian carcinoma.[252] The hyperthermic intraperitoneal chemotherapy was effective in ovarian cancer treatment[253] and resulted in a faster wound healing after abdominal surgeries than that of using chemotherapy alone.[252] Various in vitro and in vivo studies have indicated the therapeutic and anticancer effects of water bath heat treatment (as a kind of whole-body hyperthermia treatments) for example at 43.5 °C and 45 °C (30 min),[254] 47 °C and 37 °C (1 min heat shock),[255] 37, 39, and 37 °C (24-hr).[256] As a novel option for cancer patients, combining hyperthermia and chemotherapy at considerably reduced-drug doses can indicate an exceptional efficacy, for example, therapy of breast cancer[249] and ovarian cancer[257]. Further, clinical experiences have indicated a combination treatment of radiotherapy with chemotherapy as a desired therapy for superficial tumors, including skin carcinomas, Merkel cell carcinoma, and malignant melanoma.[244] In addition to the mentioned treatments, combined therapy methods such as hyperthermia, chemotherapy, and immunotherapy can be used in the prospective studies.

In vitro Studies on Magnetic Nanocomposites for Hyperthermia and Cancer Therapy

MNCs are gaining attention in smart and remotely guided drug delivery systems owing to their magneto effects and guide-ability by EMF, heating capability under AMF, and visualization properties for monitoring their pharmacokinetics. With implantable and/or external EMF, drug-loaded MNCs can operate the targeted actions and time-controlled drug release inside the body for guided treatment of cancer cells. Therefore, there are plenty of room for novel multifunctional drug-loaded MNCs in tumor targeting that EMF and MHT can potentially improve targeting actions and anticancer effects.[258,259] Anticancer drugs are basically conjugated onto MNCs via chemical and/or physical binding methods. Physical binding is facile and achieved through the hydrophilic/hydrophobic, host-guest self-assembly, electrostatic, and affinity interactions.[260] Chemical binding is obtained from the chemical interaction between the drug molecules and surface of MNCs with various functional groups such as carboxyl, amino, and thiol. Table 5 summarizes the studies devoted to various MNCs for in vitro targeted drug delivery and MHT.

An interesting MNCs was fabricated via using pH/thermo-sensitive polymer of poly(2-(dimethylamino)ethyl methacrylate) to coat MNPs for dual response in controlled drug delivery systems.[217] In a recent study,[233] round-shaped SPIONs (~15 nm) (Figure 6a) was homogeneously coated with citric acid (2 nm thickness) abbreviated as SPION@CA (Figure 6b) for delivering DOX (SPION@CA-DOX) (Figure 6c) and epirubicin (SPION@CA-epirubicin) (Figure 6d). As presented in Figures 6c and d, drug loading did not damage the structure and morphology of the MNCs. In a study by Wang et al,[204] DOX-Fe_3O_4@agar PMNCs (Figure 6e–k) with an average size of 9.2±3.2 nm (Figure 6e) and *Ms* of 41.9 emu/g (Figure 6f) showed a magnetocaloric temperature of 43 °C under AMF only after 5 min (Figure 6h), whereas it indicated a maximum drug release rate of 85±3% after 56 min at pH 7 to simulate the intestinal environment (Figure 6g). Figure 6i indicates the schematic illustration of DOX-Fe_3O_4@agar for eliminating HT-29 cancer cells under AMF that the red fluorescence was found in the image of HT-29 cell treated with DOX-Fe_3O_4@agar for 1-hr (Figure 6j). Then, the release of DOX caused 44% and 86.6% cancer cell death without and with applied AMF, respectively (Figure 6k). The SAR value of DOX-Fe_3O_4@agar increased considerably with increasing AMF

Table 5 Overview of Some Recent in vitro Studies on MNCs for MHT and Targeted Drug Delivery Systems

Magnetic Nanoagent	Type of Analysis, Size (nm)	Loaded Drug	Drug Release	Origin, Type, Cell Lines	Results	Ref.
Monoclonal antibody conjugated Fe_3O_4	TEM, 36	DOX	~60% release at pH 5.0 medium with AMF	Gastric, cancer, GTL-16	Chemotherapy and combined therapy caused 20% and 78% cancer cell death, respectively	[261]
Silica-Fe_3O_4	TEM, ~ 30	Maytansinoid	Nr	Macrophage, cancer, IC21	Chemotherapy, MHT, and combined therapy caused 20%, 15%, and 78% cancer cell death, respectively	[262]
Oleosome-$ZnFe_2O_4$	TEM, ~80	Carmustine	~4% and ~23% release at pH 7.2 medium without and with AMF, respectively	Breast, cancer, SK-BR-3	Chemotherapy, MHT, and combined therapy caused 60%, 40%, and 80% cancer cell death, respectively	[263]
Fe_3O_4@agar	TEM, 9.2	DOX	85% release at pH 7.0 medium	Colon, cancer, HT-29	Combined therapy caused ~85% cancer cell death	[204]
$MnFe_2O_4$/ω-hydroxyacid-co-poly(d,l-lactic acid)	DLS, 160	Paclitaxel	~98% release within 18 days at 7.4 medium	Colon, cancer, Caco-2 and hASCs	The elimination of cancer cell was dose-dependent and significantly increased after treatment with increasing sample concentration (1000 μg/mL)	[264]
Malic acid/Fe_3O_4	TEM, 9.2	DOX	~79% release at pH 6.5 medium. ~22% release at pH 7.4 medium	Breast, cancer, MCF-7	65% cancer cell death without AMF	[265]
Magnetic nano/micro-particles based on clinoptilolite-type of natural zeolite	SEM, 75	Nr	Nr	Nr	The temperature in the MCZ injected chicken wing is increased from 27.5 °C to 32.1 °C in 5 min and to 39.7 °C in 22 min with AMF	[266]
Mn0.5Zn0.5Fe2O4@PEG nanofluid	TEM, 6.5	Nr	Nr	Retinal, cancer, ganglion	Controlling the recovery time during MHT affects the cell death rate	[267]
$CuFe_2O_4$	TEM, 17.3	Nr	Nr	Colon, cancer, HT-29	53% cancer cell death without AMF	[213]
Graphene oxide/ $CoFe_2O_4$	TEM, 5	Nr	Nr	Breast, cancer, MCF-7	42% and 70% cancer cell death without and with AMF, respectively	[268]
PVA-Mg-Co-Fe_2O_4	DLS, <120	5FU	Nr	Breast, cancer, MCF-7 and cervical, cancer, HeLa	>65% cancer cell death without AMF	[269]

(*Continued*)

https://doi.org/10.2147/IJN.S375964

Table 5 (Continued).

Magnetic Nanoagent	Type of Analysis, Size (nm)	Loaded Drug	Drug Release	Origin, Type, Cell Lines	Results	Ref.
Chitosan/Fe_3O_4	SEM, 125	5FU	45% release at pH 7.4 medium	Glioblastoma, cancer, A-172	25% cancer cell death with AMF and no significant elimination of normal cells fibroblasts	[207]
$Fe_{3-\delta}O_4$@silane and a thermoresponsive copolymer shell composed of 2-(2-methoxy) ethyl methacrylate and oligo(ethylene glycol) methacrylate moieties (1.14 mL)	TEM, 10	DOX	100% release after 52-hr at 42 °C and pH 7.4 medium. 62% release after 52-hr at 37 °C and pH 7.4 medium	Ovary, cancer, SKOV-3	~70% cancer cell death at 41 °C	[209]
$Fe_{3-\delta}O_4$@silane and a thermoresponsive copolymer shell composed of 2-(2-methoxy) ethyl methacrylate and oligo(ethylene glycol) methacrylate moieties (1 mL)	DLS, 55–80	DOX	100% release after 52-hr at 42 °C and pH 7.4 medium. 70% release after 52-hr at 37 °C and pH 7.4 medium	Nr	Nr	[209]
Graphene quantum dots/Fe_3O_4/SiO_2	Nr	DOX	30% and 45% release at pH 5.0 medium with 37 °C and 50 °C, respectively	Breast, cancer, 4T1	18%, 80%, and 92% cancer cell death without, with AMF one, and two times, respectively. Chemotherapy, MHT, and combined therapy caused 40%, 65%, and 80% cancer cell death, respectively	[210]
Graphene quantum dots/Fe_3O_4/SiO_2	TEM, 100	Nr	Nr	Breast, cancer, 4T1	44% and 52% cancer cell death without and with AMF, respectively.	[210]
Fe_3O_4/MamC/proteinAR-3 mAbs (IgG1)	TEM, 36	DOX	44% and 25% release at pH 7.4 medium with and without AMF. 6% and 2% at pH 5.0 medium with and without AMF	Colorectal, cancer, HT-29	7% and 18% cancer cell death without and with AMF, respectively	[211]
$La_{0.7}Sr_{0.3}MnO_3$/PEG	TEM, 15–20	DOX	46% and 14% release at pH 5 and 7.4 medium without AMF, respectively	Breast, cancer, MCF-7	29% and 90% cancer cell death without and with AMF, respectively	[270]
Human serum protein/$La_{0.7}Sr_{0.3}MnO_3$/PEG	Nr	DOX	39% and 12% release at pH 5 and 7.4 medium without AMF, respectively	Breast, cancer, MCF-7	16% and 79% cancer cell death without and with AMF, respectively	[270]
Alginate-chitosan-Fe_3O_4	TEM, ~14	DOX	22.5% and 0.2% release in tumor site with and without AMF, respectively	Breast, MCF-7	Chemotherapy, MHT, and combined therapy caused 85%, 63%, and 95% cancer cell death, respectively	[212]

ZIF-90 on polydopamine-coated Fe_3O_4	SEM, 200	DOX	17.3%, 70.8%, and 88.7% release at pH 7.4, 6.0, and 4.5 medium after 24 h, respectively	Cervical, cancer, HeLa	Chemotherapy, MHT, and combined therapy caused 32%, 50%, and 72% cancer cell death, respectively	[271]
Ferumoxytol-medical chitosan	Nr	DOX	~100% drug release at 43 °C and pH 5.2 medium	Colon, cancer, HT-29	Chemotherapy, MHT, and combined therapy caused 32%, 50%, and 72% cancer cell death, respectively	[272]
Lipid based Fe_3O_4	TEM, ~50	Temozolomide	61.3% and 100% at pH 7.4 and 4.5 medium after 7 days with AMF	Glioma, cancer, Uppsala 87	Chemotherapy, MHT, and combined therapy caused 10%, 44%, and 50% cancer cell death, respectively.	[273]
IONPs stabilized with trimethoxysilylpropyl-ethylenediamine triacetic acid as a carrier of DOX	TEM, 4.76	DOX	40% and 65% release within 2-hr at pH 7 and 5 medium, respectively	Mouse brain-derived microvessel endothelial, bEnd.3, Madin–Darby canine kidney transfected with multi-drug resistant protein 1 (MDCK-MDR1), and human U251 GBM cells	The combination of magnetic enhanced convective diffusion and the cadherin binding peptide for transiently opening the blood–brain barrier tight junctions are expected to enhance the efficacy of cell death (over 90%) within 48-hr of treatment using the DOX-EDT-IONPs	[274]
PEG coated $NiFe_2O_4$	TEM, 55	DOX	Release rate of 1.33% per min.	Nr	Nr	[275]
IONPs/PLGA fiber	TEM, 600 nm fiber and 20 nm IONPs	Bortezomib	18% and 70% release at 7.4 and 5.5 medium.	Fibroblast, cancer, NIH3T3 and mouse mammary carcinoma, 4T1	Many of the cells exhibited a shrunken morphology with membrane blebbing on their surface	[276]
Lectrospun chitosan/cobalt ferrite/titanium oxide nanofibers	SEM, 110	DOX	~85% and ~52% release at 5.3 and 7.4 medium with AMF. ~63% and ~40% release at 5.3 and 7.4 medium without AMF	Melanoma, cancer, B16F10	78% cancer cell death with AMF	[277]

(*Continued*)

https://doi.org/10.2147/IJN.S375964 DovePress

Table 5 (Continued).

Magnetic Nanoagent	Type of Analysis, Size (nm)	Loaded Drug	Drug Release	Origin, Type, Cell Lines	Results	Ref.
Graphene Oxide-Fe_3O_4-PEG	TEM, ~20	DOX	~58% and ~19% release at 5 and 7.4 medium without AMF	Murine, cancer, colorectal, CT26	80% cancer cell death with AMF	[219]
PLGA/Fe_3O_4	TEM, 172.1	DOX	Nr	Colon, cancer, CT26	~80% cancer cell death with AMF	[220]
$Mg_{0.13}$-Fe_2O_3	TEM, 7	Nr	Nr	Glioblastoma, cancer, U87MG	75% and 100% cancer cells death at a temperature of 48.4 °C and 63.5 °C with AMF, respectively	[278]
Ether triad modified core-shell magnetic mesoporous silica	TEM, 50–60	DOX	55.3%, 73.5%, and 85% release at pH 6.5, 5.0, and 4.0 medium, respectively, after 24-hr without AMF. 3.6%, 4.5% and 6.2% release at 25 °C, 37 °C, and 45 °C in pH 7.4 medium without AMF. 80%, 88%, and ~ 95% release at 25 °C, 37 °C, and 45 °C, respectively, at pH 7.4 medium with AMF.	Breast, cancer, MDA-MB-231	~5% and 77% cancer cell death without and with AMF, respectively	[279]
Fe_3O_4@PLA-grafted P (HEMA-co-MAA-co-NIPAAm-coTMSPM)	SEM, 96	DOX, Methotrexate	40% MTX and 75% DOX release at 41 °C in pH 4 medium after 6 days	Nr	Nr	[280]
Poly(Nisopropyl acrylamide-co-acrylic acid)-co-AAc)@mSiO_2@Fe_3O_4	TEM, ~100	5FU	7.8% and 47% release after 20-hr with AMF at 37 °C and 45 °C, respectively	Nr	Nr	[89]
IONPs - (poly(maleic anhydride-alt -1-octadecene)- (tetramethylrhodamine 5(6)-carboxamide cadaverine - N-(3 dimethylaminopropyl)-N′-ethylcarbodiimide hydrochloride - 4-aminophenyl β-D glucopyranoside	TEM, ~11	Nr	Nr	3D pancreatic, cancer tumor, MIA PaCa-2	72% cancer cell death with AMF	[226]
Chitosan coated Fe_3O_4	TEM, 30–40	Nr	Nr	Lung, cancer, A549	50–70% cancer cell death with AMF	[228]

Graphene oxide - Fe_3O_4	TEM, 10–21	Nr	Nr	Lung, cancer, A549	80.5% cancer cell death with AMF	[85]
Silica coated lanthanum strontium manganese oxide	TEM, 35	Nr	Nr	Lung, cancer, A549	~75% cancer cell death without AMF	[229]
Chitosan-g-N-isopropylacrylamide coated magnetic-silica	TEM, 30–50	DOX	83.30% release after 5-hr with AMF at 45 °C and pH 4.0	Neck, cancer, Cervical	90.83% cancer cell death with AMF	[230]
Trimesic acid coated SPIONs dispersed in triethylene glycol	TEM, 9	Nr	Nr	Breast, cancer, MCF-7	90% cancer cell death with AMF	[231]
Tetraethyl orthosilicate coated $La_{0.7}Sr_{0.3}MnO_3$	TEM, 45	Nr	Nr	Lung, cancer, A549	80% cancer cell death with AMF	[232]
Cetyltrimethylammonium bromide and polycaprolactone coated Fe_3O_4	TEM, 21	Nr	Nr	Liver, cancer, HepG2	~60% cancer cell death with AMF	[235]
$CoFe_2O_4$	TEM, ~10	Nr	Nr	Mouse fibroblast, normal, L929	15% normal cell death without AMF, showing high biocompatibility	[193]
Oleic acid/PEG coated $CoFe_2O_4$	TEM, ~10	Nr	Nr	Mouse fibroblast, normal, L929	0% normal cell death with AMF, showing high biocompatibility	[193]
$Co_{0.03}Mn_{0.28}Fe_{2.7}O_4/SiO_2$	TEM, ~22	Nr	Nr	Osteosarcoma, normal, MG-63 and MEF	Less than 3% normal cell death without AMF, showing high biocompatibility	[198]
Contractible hydroxypropyl methyl cellulose/Fe_3O_4 hydrogel	TEM, 200	DOX	57.6% and 32.3% release with and without AMF in 24-hr at pH 7.4 medium. 78.8% and 41.7% with and without AMF at pH 5.5 medium	4T1 breast cancer	No tumor recurrences occurred in the chemo-thermal therapy group after 21 days of MHT	[207]
Fe3O4 NPs-silica-poly(Nisopropyl acrylamide-co-acrylic acid)	Nr	5FU	7.8% and 47% release after 20-hr at 37 °C and 45 °C, respectively	Nr	Nr	[89]
IONPs coated with graphite-like shell and labeled with Alexa 647 fluorescent marker	Nr	Nr	Nr	Nr	With an applied field of 38 kA/m at 980 kHz, tumors could be heated to 60 °C in 2 minutes, durably ablating them with millimeter (mm) precision, leaving surrounding tissue intact	[281]

https://doi.org/10.2147/IJN.S375964

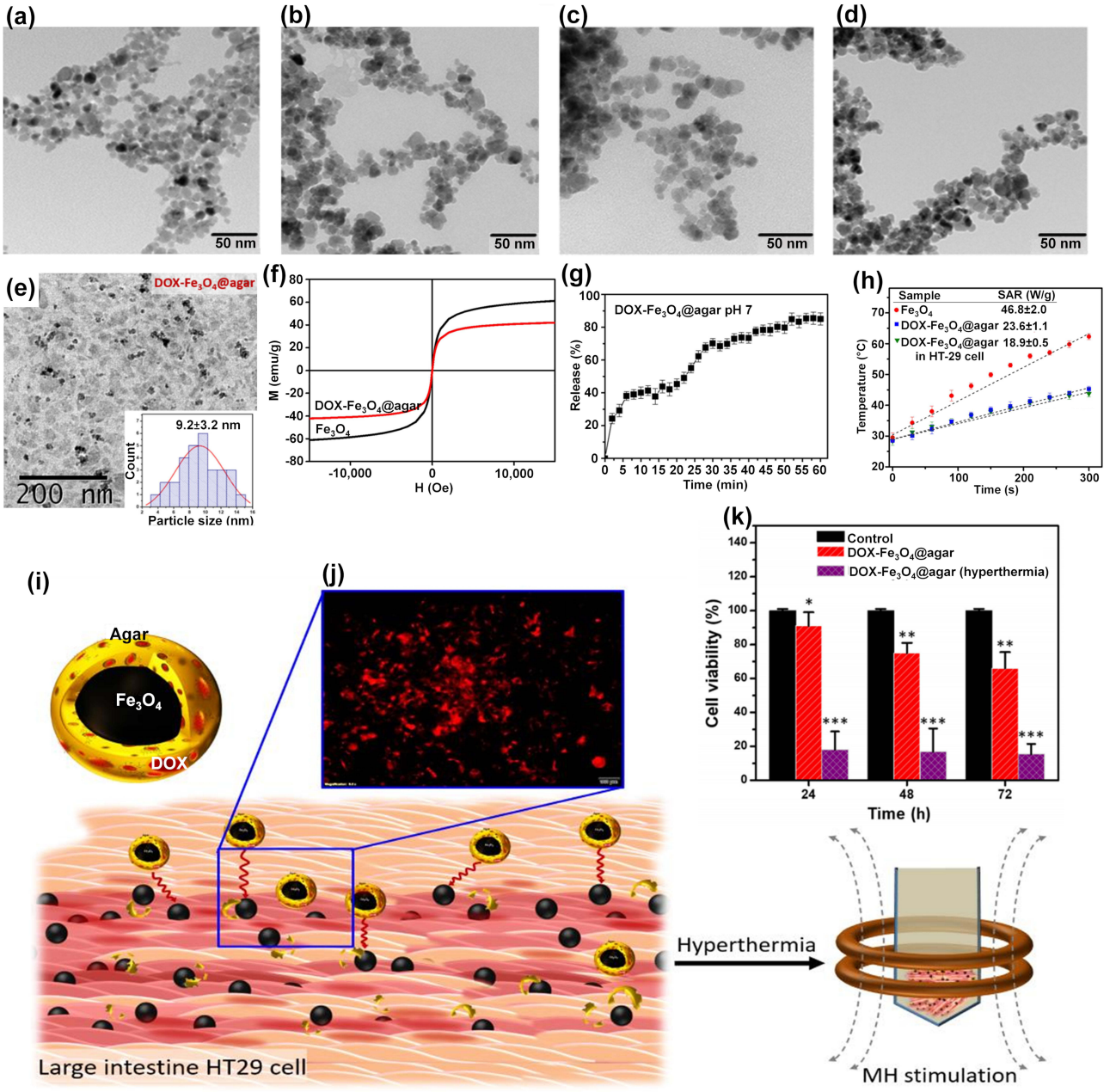

Figure 6 TEM images of (**a**) SPIONs, (**b**) SPION@CA, (**c**) SPION@CA-Dox, and (**d**) SPION@CA-epirubicin.[233] (**e**) TEM image and the particle size distribution analysis of DOX-Fe_3O_4@agar, (**f**) Magnetic strength of Fe_3O_4 and DOX-Fe_3O_4@agar, (**g**) Drug release profiles of DOX-Fe_3O_4@agar at pH 7, (**h**) The SAR values and temperature achieved by Fe_3O_4, DOX-Fe_3O_4@agar, and DOX-Fe_3O_4@agar in HT-29 cells under applied AMF (applied field = 400 A, frequency = 250 kHz), (**i**) Schematic of effects of DOX-Fe_3O_4@agar for eliminating HT-29 cancer cells under hyperthermia, (**j**) fluorescence microscopy images of HT-29 cells after 1-hr of incubation with DOX-Fe_3O_4 @agar, and (**k**) Cell survival of HT-29 cells treated by DOX-Fe_3O_4@agar with and without MHT.

Notes: The significance levels denote as * ($p < 0.05$), ** ($p < 0.01$), and *** ($p < 0.001$) indicate the degree of statistical significance when compared to the control group. (i, j, and k) Reprinted from Wang Y-J, Lin P-Y, Hsieh S-L, et al. Utilizing edible agar as a carrier for dual functional doxorubicin-Fe3O4 nanotherapy drugs. *Materials*. 2021;14 (8):1824. Creative Commons.[204]

strengths owing to the heating loss mechanisms, similar to different reports on Fe_3O_4[19,20] and polycaprolactone-coated Fe_3O_4,[235] γ-Fe_2O_3,[285] and CoMn IONPs.[286] In another study,[287] Parekh et al used a surfactant of the small-chain fatty acid-coated IONPs to trigger temperature sensitivity, and subsequently 75% of HeLa cancer cell death under 24-hr exposure to AMF. In a different study,[80] a novel and low-cost PMNCs were fabricated using Fe_3O_4 nanofillers supported on rice straw cellulose fibers in 5FU drug delivery systems. It showed the pH and thermo-sensitive drug release and increased selectivity and anticancer activities towards colorectal cancer cell lines in 2D monolayer and 3D tumor spheroid models under EMF and heat induction of 44.2 °C.[80] In

Table 6 The in vivo Studies on MNCs for MHT and Targeted Drug Delivery

Magnetic Nanoagent	Type of Analysis, Size (nm)	Loaded Drug	Drug Release	Cell Lines	NP Administration Route, Animal Model	Results	Ref.
PLGA/Fe_3O_4	TEM, 172	DOX	Nr	CT26 colon cancer in 5 mice	Intratumoral injection, Mouse	The tumor size decreased 4 times with AMF	[220]
Commercially available "biocompatible" type of MNPs	TEM, 15	Nr	Nr	Nr	Injected intravenously via a tail vein, Mouse	By direct intratumoral injection of MNPs, tumor size decreased 60% in 14 days (amount of Fe ~17 mg). In addition, 5 out of 5 mice were tumor free at 120 days. They had an initial tumor size of 1.5 cm (amount of Fe ~6 mg + injections for retreatment).	[282]
Commercially available "biocompatible" type of MNPs	TEM, 11	Nr	Nr	OVCAR-3 ovarian tumor cells	Injected intravenously via a tail vein, Mouse	7 out of 9 (78%) tumor free after 160 days	[282]
Fluorescent IONPs/PLGA conjugated with human epidermal growth factor receptor 2	DLS, 524	Gemcitabine	23% release in 5 minutes at 440 kHz frequency (16.27 kA/m) and sustained drug release for 11 days	MIAPaCa-2 in SCID mice	Intravenous injection, Mouse	The tumor regression study at the end of 30 days showed significant tumor regression (86±3%) with MHT	[225]
Mg0.13-Fe2O3	TEM, 7	Nr	Nr	Hep3B xenografted animal models	Injected into the tumor directly, Mouse	It was clearly observed that the tumor was completely killed after 2 days with AMF.	[278]
Fe3O4/Poly(ethylene glycol) methyl ether	SEM, 73	Nr	Nr	Nude mice xenografted with breast cancer MCF-7	Injected into the tumor directly, Mouse	Following treatment, the tumor volumes were monitored for up to 40 days. For the control mice, tumor size increased 25 fold by the fortieth day. With AMF (1.2 × 109 A m^{-1} s^{-1}), from the sixth day onwards, tumors were completely eliminated without recurrence within the experimental period	[283]

(*Continued*)

https://doi.org/10.2147/IJN.S375964 DovePress

Table 6 (Continued).

Magnetic Nanoagent	Type of Analysis, Size (nm)	Loaded Drug	Drug Release	Cell Lines	NP Administration Route, Animal Model	Results	Ref.
Biomimetic magnetic NPs mediated by magnetosome proteins	TEM, 36	DOX	100, 300, and 500 μg of BMNPs were exposed at (130 kHz and 18 kA m^{-1}) for 20 min	4T1 and MCF-7 in Balb/c female mice of about six weeks old	Tail-vein injection, Mouse	Around 40% of the tumor size decreased by MHT and chemotherapy, which was higher than chemotherapy alone.	[284]
Graphene oxide-cobalt ferrite	TEM, 5	Nr	Nr	MCF7	Injected in situ to the multiple points of the tumor, Mouse	BALB/c mice and the results indicated the smaller size of the tumor with the concentrations of 0.001 and 0.002 gr/mL and the respective magnetic frequencies of 400 and 250 kHz for 10 min after 27 days	[268]
IONPs-(poly(maleic anhydride-alt -1-octadecene)-(tetramethylrhodamine 5(6)-carboxamide cadaverine-N-(3 dimethylaminopropyl)-N′-ethylcarbodiimide hydrochloride-4-aminophenyl β-D glucopyranoside	TEM, ~11 DLS, ~85	Nr	Nr	Pancreatic tumor cell line (MIA PaCa-2)	Intratumoral injection, Rat tail	~47% and ~14% antitumor effects in heterotopic xenograft mouse model with and without AMF, respectively.	[226]

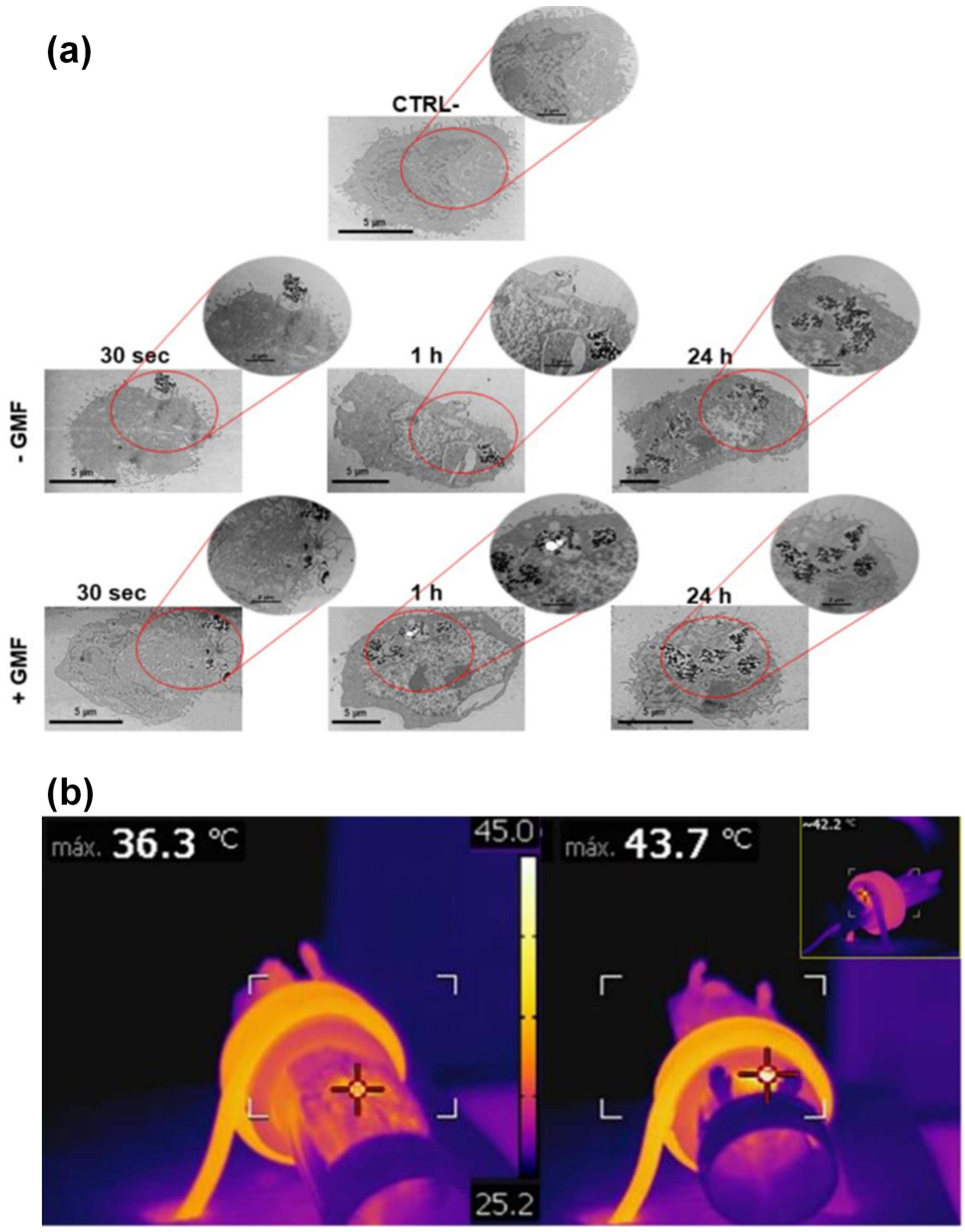

Figure 7 (**a**) Interaction of BMNPs with 4T1 cells in the presence/absence of a continuous gradient magnetic field analyzed at TEM, micrographs of the cells incubated with the 100 μg/mL of BMNPs for different periods of time. The micrographs are representative of alternate serial cuts of the cell pellets of each sample. Scale bar, 5 μm. (**b**) In vivo antitumor activity of BMNPs under the influence of AMF, Images were captured using a thermic camera of a representative mouse without (left) and with (right) injected BMNPs during AMF treatment. Note the different colors within the circle on the backside of the mouse.[284]

conclusion, the use of polymers as coating or solid supports in MNCs is one of the key points shown by various studies on magnetic drug composites for possible clinical settings of MHT and magnetic targeting in future.

In vivo Studies on Magnetic Nanocomposites for Hyperthermia and Cancer Therapy

The therapeutic nature of MNCs with the arsenal of magnetothermal drug delivery systems has manifested several advantages over the conventional cancer therapy methods due to their low damage to normal cells and ability to deliver sufficient drug dosage to the tumor. Various studies have recommended the use of MHT and magnetic targeting as an efficient anti-tumoral therapy for in vivo studies using animal models. This can be done through intravenous injection of MNCs (with or without loaded-drug) in tumor site under EMF to guide MNCs onto the targeted tissue and then inducing AMF to selectively heat the tumor and control the drug release for effective elimination of cancer cells without harmful damages for normal cells. Table 6 summarizes the in vivo studies on different MNCs for MHT and targeted drug delivery systems.

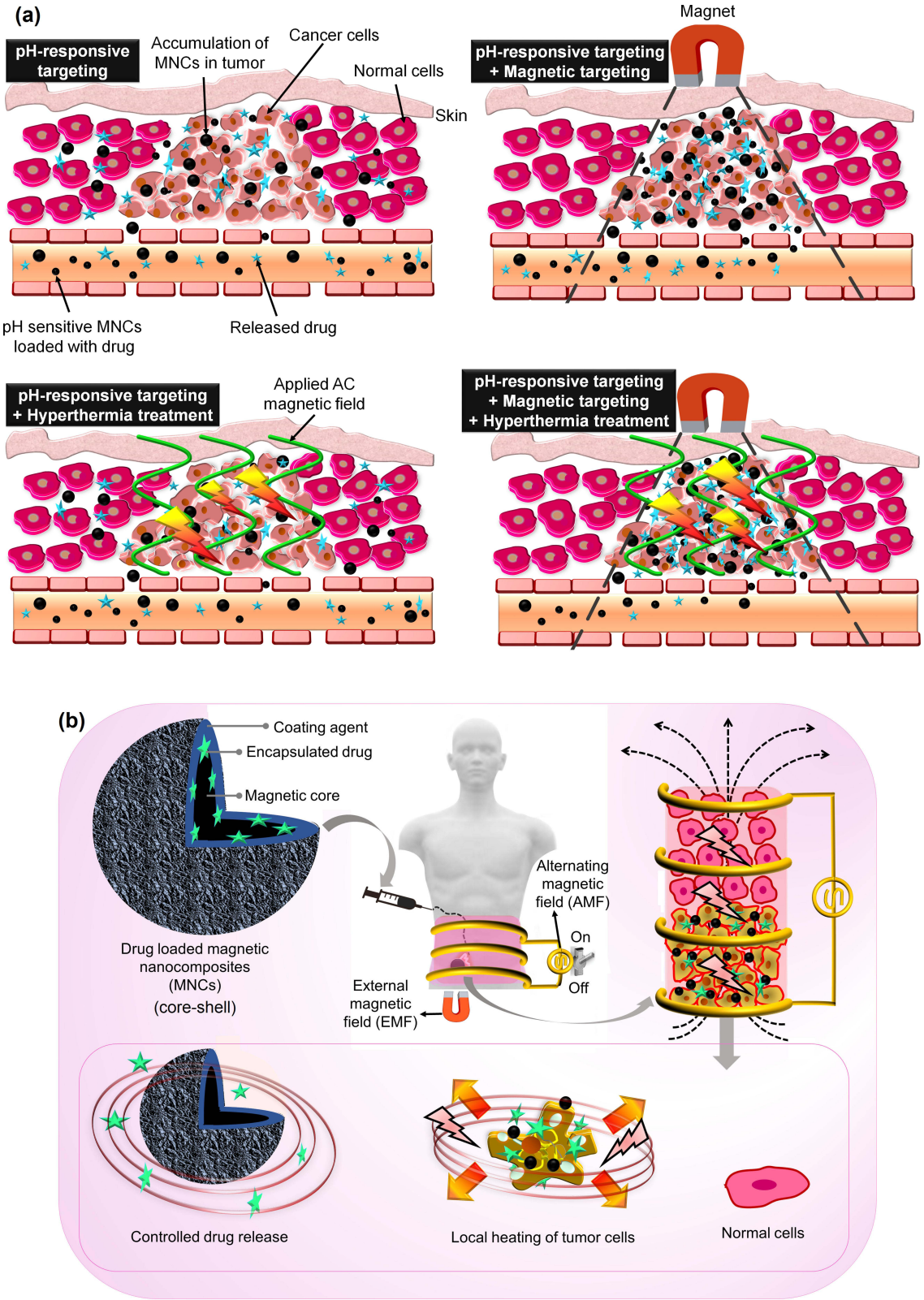

Figure 8 (**a**) Schematic of pH, magneto, and thermo-responsive drug delivery systems using drug-loaded MNCs. (**b**) The schematic of prospective use of drug-loaded MNCs for hyperthermia and magnetic targeted cancer therapy.[220,318]

Thermo-chemosensitization means increasing the temperature for the enhancement of drug cytotoxicity to obtain advanced cancer treatment. Oltolina et al[284] successfully encapsulated anticancer drug DOX onto biomimetic MNPs (BMNPs) via the succor of magnetosome proteins for both in vitro and in vivo MHT of breast cancer model (Figure 7a and b). From the TEM images at various time points, the interaction of BMNPs with 4T1 cell membrane internalized under applied magnetic field. In addition, DOX-BMNPs with AMF-induced hyperthermia decreased the size and weight of the tumor, proving that hyperthermia successfully enhanced targeted drug release to obtain potent antitumor actions.

In a study by Garanina et al,[281] hydrochloric acid treatment was used to coat the iron core NPs followed by additional layers of onion-like carbon coating (Fe@C core-shell NPs) to save the iron core from oxidation. With the presence of a constant magnetic field (150 mT), the magnetic characteristics of superparamagnetic Fe@C core-shell NPs and their endocytosis process through living tumor cells were analyzed. According to the results of correlative light and electron microscopy, the microstructure of Fe@C core-shell NPs was maintained even after internalization by the living cells. Alignment of internalized Fe@C core-shell NPs and their magneto controllability were achieved by exposure to the magnetic field and long-term observation using a confocal microscope revealed that the biocompatibility of the magnetic sample was attributed to carbon onion-like shells. Therefore, Fe@C core-shell NPs were safe without toxicity towards the cell physiology and did not trigger apoptosis.

Biodegradation of Magnetic Nanocomposites in the Body

The safety of MNCs in medical application is associated with i) short-term stability such as their blood circulation time and tissue or organ biodistribution and ii) long-term effects, including their toxicity, degradation, and clearance from the body.[288] In the blood circulation, stability of MNCs can vary from minutes to several days and is characterized by their surface coating and the composition of the protein corona.[289,290] The excess MNCs mostly accumulated in the liver and spleen, and are removed from the bloodstream.[291,292] In regard to the long-term effects, factors such as the rate of metal ion release, iron scavenges from the iron metabolic protein compound, formation of ferritin via gradual transition of the particles, and the degradation effects for potentially de novo particle fabrication play the important roles.[293] It was reported that MNCs with diverse magnetic core structure and counterparts have negative impact on the long-term pharmacokinetics.[288]

It should be noted that the human body's iron content is presented in transferrin (0.1%), ferritin (15–30%), and myoglobin (4%), and within hemoglobin protein (65%).[294] The intracellular degradation of IONPs has a comparable mechanism with those of ferritin. After the degradation of IONPs, the main iron-protein complexes of ferritin (hydrodynamic size ~13 nm) and transferrin support the storage and transport of the iron ions in the body, respectively.[295] The lysosomal proteases cause the dissolving of the protein shell around ferritin and subsequently, the internal iron ions are degraded in the acidic condition of the lysosomes. This leads to the presence of extra iron in the body, which is regulated by the inherent clearance systems of the body. It was stated that the biodegradation of MNCs can be more attributed to the initial intracellular amount of MNPs compared to the coating itself.[296] The coating and surface modification of MNCs advantageously decrease the water penetration to increase the degradation time in the macrophages. The size of MNCs may influence the surface chemistry, charge, and the bioavailability of the particles in the human body.[297–299] It was stated that the various drug nanocarriers such as MNCs with sizes between 10 and 100 nm trigger longer half lives in the blood and can also go through capillaries.[300] Circulation of the plasma transferrin triggers the transfer of iron to different areas of the body. The liver and spleen are responsible for the clearance of NPs from the bloodstream.[301] Renal clearance might remove the particles with sizes below 5–7 nm,[302] however, particles with sizes above 5 microns may result in capillary blockage.[303] It should be noted that the excess MNPs get accumulated in tissues including lung and adipose tissue, which may cause unwanted toxicity.[304] It is still required to analyze the toxicity, biodistribution, biodegradation, and clearance of different new MNCs via short and long time evaluation for advanced anticancer drug delivery nanosystems.

Future Perspectives in the Use of Magnetic Nanocomposites

MNCs as multifunctional carrier systems can be externally guided by EMF and produce heat by AMF for the multi-stage and on-demand drug release procedures.[4,80] Figure 8a schematically shows the magneto, pH, and thermoresponsive drug delivery systems using drug-loaded MNCs. Figure 8b indicates the schematic of prospective use of drug-loaded MNCs

for hyperthermia and magnetic targeted cancer therapy. Several studies have reported that the long-term accumulation of nanocarriers can lead to unwanted toxicity, health risks, and harmful side-effects such as oxidative stress, fibrosis, inflammation, genotoxicity, and subsequently cell death.[305] Although MNPs may potentially penetrate the blood–brain barrier and generate the iron imbalance causing Alzheimer's and Parkinson's disease[41,42], they can be effectively removed through their high magnetization and guideability following the drug release in the body.[306,307] This can decrease the long-term NPs accumulation and unwanted damage to the human body.[40] To achieve this, there are several important considerations. First, a direct method can be applied using needles inserted into the target tumor for the administration of drug-loaded MNCs. Second, EMF can magnetize the tip of the needle to effectively direct and deliver the drug-loaded MNCs to the target tumor. Third, it is necessary to understand the performance and mechanisms of the drug release in the distributed tumor tissues and organs. Fourth, the use of magnetic targeting systems can clear MNCs from the body to minimise the side effects in the targeted tissue and body.[308] In targeted therapy, particles penetrate tissues from capillaries, such that strong magnetic fields are needed to maintain MNCs in large arteries since the blood flow decreases the accumulation of magnetic carriers at the target tissue.[43] In particular, the velocity of blood flow in the capillaries (±0.5 cm/s) is 50–100 times lower than the linear velocity of blood in large arteries. A different matter related to magnetic carriers is obtaining the desired depth penetration of the magnetic field towards the target area. Since the magnetic field decreases with distance, it is challenging to transfer MNCs near the target areas within the body with depth more than 2 cm from the skin.[43] Importantly, the higher interstitial fluid pressure in tumors (10–30 mmHg) than that in the healthy tissue (1–3 mmHg)[309] prevents convective flow from the vasculature into the interstitial tissue as can be limited even if the extracellular matrix of tumors has a pore size around hundreds of nanometers.[310,311] Therefore, MNCs penetration into the tumor mainly reflects the level of MNCs diffusion,[312] and delivering the NPs onto the tumor is mostly limited to perivascular areas. Noticeably, without convection for heat transfer using the bulk motion of a fluid, the larger NPs move slowly over the extracellular matrix, causing ineffective tumor therapy. For instance, 100 nm micelles indicated a lack of tissue penetration and subsequently lower therapeutic effect than 30 nm micelles.[313] Thus, the efficiency of tumor therapy is strongly linked to increased NPs penetration into tumors, which can be obtained via using smaller NPs[314]. It is worth to mention that bigger particles are more strongly attracted by EMF. Thus, in magnetically guided drug delivery systems, the size of MNCs should satisfy both tissue penetration efficiency and attraction to the magnet. Due to the transparency of body tissues to EMF, magnetophoresis is considered as a bioorthogonal probe for improving NPs accumulation and penetration into the tumor. It is reported that the magnetic effect of an applied single EMF only from one side would be quickly reduced with distance since the single EMF is effective for magnetophoresis with only less than a 5 mm distance from the tumor.[315] Deeper body tissues can be targeted by catheter-related magnetophoresis methods using steering coils to guide MNCs to reach the tumor vasculature. The underlying limitation of this strategy is its invasive procedure as the catheter must be physically steered to reach the tumor area.[316] This challenge has been tackled by using two oppositely polarized EMFs to enhance the accumulation and subsequence penetration of MNCs into the targeted solid tumors[316,317]. The two oppositely EMFs polarized form a zero point at the middle of the configuration for delivering MNCs onto the solid tumors, even at the deep tissues. EMF can improve the accumulation of magnetoliposomes for an effective inflammation process. In addition, it can decrease the amount of iron located in the plasma, liver, and spleen of mice.

Due to the practical problems and difficult process, there have been very limited reports on the application of magnetic drug delivery systems in humans. An example of a human trial after successful animal experiments is a study on 14 patients with colon adenocarcinoma or hypernephroma.[320] These patients were given epirubicin-loaded ferrofluids with a size below 100 nm via intravenous injection and guided through EMF (0.8 T). There was around 0.5 cm distance between EMF and the surface of the tumor. It was shown that 120 min of EMF exposure was sufficient to localize MNPs to obtain magnetic resonance spectroscopy (MRS) and histology. In another study, MHT in combination with both radiation and chemotherapy was accomplished for 22 patients affected by recurrent tumor entities,[321] of which all patients responded and tolerated the applied heat treatment well.

It was mentioned earlier that the carriers with single functionality could respond to only one external or internal drug release procedure. As can be understood from Figure 8, anticancer drug-loaded pH-sensitive MNCs under AMF and

EMF can perform a desired multifunctional therapy of which the individual hyperthermia, magnetic targeting, and chemotherapy are incapable.

MNCs have magnetothermal responses to be utilized in multimodal drug delivery systems for targeted cancer therapy in an eco-friendly manner. Magnetic targeting combined with hyperthermia therapy can tackle most, if not all, of the issues related to single-modality cancer treatments. In multi-stage cancer studies, promising results were reported for the combination therapy using MNCs, hyperthermia, and tumor pH targeting. In addition to the high drug loading capacity and therapeutic efficacy of MNCs, the external magnetic field and alternating magnetic field can be used for remotely switchable on-demand drug release and precise steering of the magnetothermal effects for local ablation of cancer cells. This comprehensive review discusses and highlights the use of MNCs in hyperthermia and targeted cancer therapy. Future studies are anticipated to scale up and generate affordable, safe, target-specific and potent MNCs for anticancer drug delivery.

Acknowledgments

This work was supported by Takasago Thermal Engineering Co. Ltd. Grant (R.K130000.7343.4B422) from the research management center (RMC) of Universiti Teknologi Malaysia (UTM) and Malaysia-Japan International Institute of Technology (MJIIT).

Disclosure

The authors report no conflicts of interest in this work.

References

1. Liu X, Zhang H, Zhang T, et al. Magnetic nanomaterials-mediated cancer diagnosis and therapy. *Prog Biomed Eng*. 2021;3:012005.
2. Sharifianjazi F, Irani M, Esmaeilkhanian A, et al. Polymer incorporated magnetic nanoparticles: applications for magnetoresponsive targeted drug delivery. *Mater Sci Eng B*. 2021;272:115358. doi:10.1016/j.mseb.2021.115358
3. Khaledian M, Nourbakhsh MS, Saber R, Hashemzadeh H, Darvishi MH. Preparation and evaluation of doxorubicin-loaded pla–peg–fa copolymer containing superparamagnetic iron oxide nanoparticles (Spions) for cancer treatment: combination therapy with hyperthermia and chemotherapy. *Int J Nanomedicine*. 2020;15:6167. doi:10.2147/IJN.S261638
4. Liao J, Huang H. Review on magnetic natural polymer constructed hydrogels as vehicles for drug delivery. *Biomacromolecules*. 2020;21 (7):2574–2594. doi:10.1021/acs.biomac.0c00566
5. Dai X, Yao J, Zhong Y, et al. Preparation and characterization of Fe3O4@ MTX magnetic nanoparticles for thermochemotherapy of primary central nervous system lymphoma in vitro and in vivo. *Int J Nanomedicine*. 2019;14:9647. doi:10.2147/IJN.S205456
6. Nasri S, Ebrahimi-Hosseinzadeh B, Rahaie M, Hatamian-Zarmi A, Sahraeian R. Thymoquinone-loaded ethosome with breast cancer potential: optimization, in vitro and biological assessment. *J Nanostructure Chem*. 2020;10(1):19–31. doi:10.1007/s40097-019-00325-w
7. Shi J, Kantoff PW, Wooster R, Farokhzad OC. Cancer nanomedicine: progress, challenges and opportunities. *Nat Rev Cancer*. 2017;17 (1):20–37. doi:10.1038/nrc.2016.108
8. Uthaman S, Lee SJ, Cherukula K, Cho C-S, Park I-K. Polysaccharide-coated magnetic nanoparticles for imaging and gene therapy. *Biomed Res Int*. 2015; 2015. doi:10.1155/2015/959175
9. Yusefi M, Chan H-Y, Teow S-Y, et al. 5-fluorouracil encapsulated chitosan-cellulose fiber bionanocomposites: synthesis, characterization and in vitro analysis towards colorectal cancer cells. *Nanomaterials*. 2021;11(7):1691. doi:10.3390/nano11071691
10. Pushpamalar J, Meganathan P, Tan HL, et al. Development of a polysaccharide-based hydrogel Drug Delivery System (DDS): an update. *Gels*. 2021;7(4):153. doi:10.3390/gels7040153
11. Dahlan N, Teow SY, Lim Y, Pushpamalar J. Modulating carboxymethylcellulose-based hydrogels with superior mechanical and rheological properties for future biomedical applications. *Express Polym Lett*. 2021;15(7). 612–625 doi:10.3144/expresspolymlett.2021.52
12. Afinjuomo F, Abdella S, Youssef SH, Song Y, Garg S. Inulin and its application in drug delivery. *Pharmaceuticals*. 2021;14(9):855. doi:10.3390/ph14090855
13. Zhang H, Neau SH. In vitro degradation of chitosan by bacterial enzymes from rat cecal and colonic contents. *Biomaterials*. 2002;23 (13):2761–2766. doi:10.1016/S0142-9612(02)00011-X
14. Narmani A, Jafari SM. Chitosan-based nanodelivery systems for cancer therapy: recent advances. *Carbohydr Polym*. 2021;272:118464. doi:10.1016/j.carbpol.2021.118464
15. Soleimani K, Derakhshankhah H, Jaymand M, Samadian H. Stimuli-responsive natural gums-based drug delivery systems for cancer treatment. *Carbohydr Polym*. 2021;254:117422. doi:10.1016/j.carbpol.2020.117422
16. Sriplai N, Pinitsoontorn S. Bacterial cellulose-based magnetic nanocomposites: a review. *Carbohydr Polym*. 2021;254:117228. doi:10.1016/j.carbpol.2020.117228
17. Yusefi M, Shameli K, Sukri SNAM. Magnetic nanoparticles in hyperthermia therapy: a mini-review. *J Res Nanosci Nanotechnol*. 2021;2 (1):51–60. doi:10.37934/jrnn.2.1.5160
18. Biedrzycka A, Skwarek E, Urban M. Hydroxyapatite with magnetic core: synthesis methods, properties, adsorption and medical applications. *Adv Colloid Interface Sci*. 2021:102401. doi:10.1016/j.cis.2021.102401

19. Hedayatnasab Z, Dabbagh A, Abnisa F, Daud WMAW. Synthesis and in-vitro characterization of superparamagnetic iron oxide nanoparticles using a sole precursor for hyperthermia therapy. *Mater Res Bull*. 2020:110975. doi:10.1016/j.materresbull.2020.110975
20. Yusefi M, Shameli K, Yee OS, et al. Green synthesis of Fe3O4 nanoparticles stabilized by a garcinia mangostana fruit peel extract for hyperthermia and anticancer activities. *Int J Nanomedicine*. 2021;16:2515. doi:10.2147/IJN.S284134
21. Herea D-D, Danceanu C, Radu E, Labusca L, Lupu N, Chiriac H. Comparative effects of magnetic and water-based hyperthermia treatments on human osteosarcoma cells. *Int J Nanomedicine*. 2018;13:5743. doi:10.2147/IJN.S174853
22. Li Y-Q, Xu M, Dhawan U, et al. Iron–gold alloy nanoparticles serve as a cornerstone in hyperthermia-mediated controlled drug release for cancer therapy. *Int J Nanomedicine*. 2018;13:5499. doi:10.2147/IJN.S163721
23. Eivazzadeh-Keihan R, Farrokhi-Hajiabad F, Aliabadi HAM, et al. A novel magnetic nanocomposite based on alginate-tannic acid hydrogel embedded with silk fibroin with biological activity and hyperthermia application. *Int J Biol Macromol*. 2023;224:1478–1486. doi:10.1016/j.ijbiomac.2022.10.236
24. Albinali KE, Zagho MM, Deng Y, Elzatahry AA. A perspective on magnetic core–shell carriers for responsive and targeted drug delivery systems. *Int J Nanomedicine*. 2019;14:1707. doi:10.2147/IJN.S193981
25. Yusefi M, Shameli K, Lee-Kiun MS, et al. Chitosan coated magnetic cellulose nanowhisker as a drug delivery system for potential colorectal cancer treatment. *Int J Biol Macromol*. 2023;233:123388. doi:10.1016/j.ijbiomac.2023.123388
26. Zhao Q, Wu Q, Ma P, et al. Selective and sensitive fluorescence detection method for pig IgG based on competitive immunosensing strategy and magnetic bioseparation. *Talanta*. 2019;195:103–108. doi:10.1016/j.talanta.2018.11.041
27. Shirejini SF, Dehnavi SM, Jahanfar M. Potential of superparamagnetic iron oxide nanoparticles coated with carbon dots as a magnetic nanoadsorbent for DNA isolation. *Chem Eng Res Des*. 2023;2023:1.
28. Nikitin M, Orlov A, Znoyko S, et al. Multiplex biosensing with highly sensitive magnetic nanoparticle quantification method. *J Magn Magn Mater*. 2018;459:260–264. doi:10.1016/j.jmmm.2017.10.078
29. Chai H, Zhu J, Guo Z, Tang Y, Miao P. Ultrasensitive miRNA biosensor amplified by ladder hybridization chain reaction on triangular prism structured DNA. *Biosens Bioelectron*. 2023;220:114900. doi:10.1016/j.bios.2022.114900
30. Ye D, Li Y, Gu N. Magnetic labeling of natural lipid encapsulations with iron-based nanoparticles. *Nano Res*. 2018;2018:1–22.
31. Li W, Fan G-C, Gao F, Cui Y, Wang W, Luo X. High-activity Fe3O4 nanozyme as signal amplifier: a simple, low-cost but efficient strategy for ultrasensitive photoelectrochemical immunoassay. *Biosens Bioelectron*. 2019;127:64–71. doi:10.1016/j.bios.2018.11.043
32. Guo A, Pei F, Hu W, et al. CdTe QDs-sensitized TiO_2 nanocomposite for magnetic-assisted photoelectrochemical immunoassay of SARS-CoV-2 nucleocapsid protein. *Bioelectrochemistry*. 2023;150:108358. doi:10.1016/j.bioelechem.2022.108358
33. Wen C-Y, Zhao L-J, Wang Y, et al. Colorimetric and photothermal dual-mode lateral flow immunoassay based on Au-Fe3O4 multifunctional nanoparticles for detection of Salmonella typhimurium. *Microchimica Acta*. 2023;190(2):57. doi:10.1007/s00604-023-05645-x
34. Lu Q, Dai X, Zhang P, et al. Fe3O4@ Au composite magnetic nanoparticles modified with cetuximab for targeted magneto-photothermal therapy of glioma cells. *Int J Nanomedicine*. 2018;13:2491. doi:10.2147/IJN.S157935
35. Darroudi M, Nazari SE, Karimzadeh M, et al. Fabrication of magnetic nanocomposite as responsive drug delivery vehicle for cervical cancer therapy. *Appl Organomet Chem*.2023;e7068. doi:10.1002/aoc.7068
36. Arsalani S, Guidelli EJ, Silveira MA, et al. Magnetic Fe3O4 nanoparticles coated by natural rubber latex as MRI contrast agent. *J Magn Magn Mater*. 2019;475:458–464. doi:10.1016/j.jmmm.2018.11.132
37. Yusefi M, Shameli K, Hedayatnasab Z, et al. Green synthesis of Fe 3 O 4 nanoparticles for hyperthermia, magnetic resonance imaging and 5-fluorouracil carrier in potential colorectal cancer treatment. *Res Chem Intermed*. 2021;47(5):1789–1808. doi:10.1007/s11164-020-04388-1
38. Li Y, Kong J, Zhao H, Liu Y. Synthesis of multi-stimuli responsive Fe3O4 coated with diamonds nanocomposite for magnetic assisted chemo-photothermal therapy. *Molecules*. 2023;28(4):1784. doi:10.3390/molecules28041784
39. Kharey P, Goel M, Husain Z, et al. Green synthesis of biocompatible superparamagnetic iron oxide-gold composite nanoparticles for magnetic resonance imaging, hyperthermia and photothermal therapeutic applications. *Mater Chem Phys*. 2023;293:126859. doi:10.1016/j.matchemphys.2022.126859
40. Mustapić M, Glumac Z, Heffer M, et al. AC/DC magnetic device for safe medical use of potentially harmful magnetic nanocarriers. *J Hazard Mater*. 2021;409:124918. doi:10.1016/j.jhazmat.2020.124918
41. Liu J-L, Fan Y-G, Yang Z-S, Wang Z-Y, Guo C. Iron and Alzheimer's disease: from pathogenesis to therapeutic implications. *Front Neurosci*. 2018;12:632. doi:10.3389/fnins.2018.00632
42. Wang J-Y, Zhuang Q-Q, Zhu L-B, et al. Meta-analysis of brain iron levels of Parkinson's disease patients determined by postmortem and MRI measurements. *Sci Rep*. 2016;6(1):1–13. doi:10.1038/s41598-016-0001-8
43. Shabatina TI, Vernaya OI, Shabatin VP, Melnikov MY. Magnetic nanoparticles for biomedical purposes: modern trends and prospects. *Magnetochemistry*. 2020;6(3):30. doi:10.3390/magnetochemistry6030030
44. Hedayatnasab Z, Abnisa F, Daud WMAW. Review on magnetic nanoparticles for magnetic nanofluid hyperthermia application. *Mater Des*. 2017;123:174–196. doi:10.1016/j.matdes.2017.03.036
45. Sanadgol N, Wackerlig J. Developments of smart drug-delivery systems based on magnetic molecularly imprinted polymers for targeted cancer therapy: a short review. *Pharmaceutics*. 2020;12(9):831. doi:10.3390/pharmaceutics12090831
46. Haniffa MACM, Munawar K, Chee CY, et al. Cellulose supported magnetic nanohybrids: synthesis, pysicomagnetic properties and biomedical applications-a review. *Carbohydr Polym*. 2021;267:118136. . doi:10.1016/j.carbpol.2021.118136
47. Makvandi P, Ghomi M, Ashrafizadeh M, et al. A review on advances in graphene-derivative/polysaccharide bionanocomposites: therapeutics, pharmacogenomics and toxicity. *Carbohydr Polym*. 2020;267:116952. doi:10.1016/j.carbpol.2020.116952
48. Lakkakula JR, Gujarathi P, Pansare P, Tripathi S. A comprehensive review on alginate-based delivery systems for the delivery of chemotherapeutic agent: doxorubicin. *Carbohydr Polym*. 2021;259:117696. doi:10.1016/j.carbpol.2021.117696
49. Jahangirian H, Kalantari K, Izadiyan Z, Rafiee-Moghaddam R, Shameli K, Webster TJ. A review of small molecules and drug delivery applications using gold and iron nanoparticles. *Int J Nanomedicine*. 2019;14:1633. doi:10.2147/IJN.S184723
50. Wu W, Wu Z, Yu T, Jiang C, Kim W-S. Recent progress on magnetic iron oxide nanoparticles: synthesis, surface functional strategies and biomedical applications. *Sci Technol Adv Mate*. 2015;16(2):023501. doi:10.1088/1468-6996/16/2/023501
51. Li H, Wang W. Preparation of diamagnetic nanoparticles under magnetic field. Google Patents; 2020.

52. Bouarissa A, Layadi A, Maghraoui-Meherzi H. Experimental study of the diamagnetism and the ferromagnetism in MoS 2 thin films. *Appl Phys A*. 2020;126(2):1–6. doi:10.1007/s00339-020-3286-1
53. Li W, Fortner JD. (Super) paramagnetic nanoparticles as platform materials for environmental applications: from synthesis to demonstration. *Front Environ Sci Eng*. 2020;14(5):1–9. doi:10.1007/s11783-020-1256-7
54. Huang P, Zhang P, Xu S, Wang H, Zhang X, Zhang H. Recent advances in two-dimensional ferromagnetism: materials synthesis, physical properties and device applications. *Nanoscale*. 2020;12(4):2309–2327. doi:10.1039/C9NR08890C
55. Hou Y, Sellmyer DJ. *Magnetic Nanomaterials: Fundamentals, Synthesis and Applications*. John Wiley & Sons; 2017.
56. Zhang H, Yang W, Cui P, Xu X, Zhang Z. Prediction of monolayered ferromagnetic CrMnI 6 as an intrinsic high-temperature quantum anomalous Hall system. *Phys Rev B*. 2020;102(11):115413. doi:10.1103/PhysRevB.102.115413
57. Surya RM, Yulizar Y, Cahyana AH, Apriandanu DOB. One-pot Cajanus cajan (L.) Millsp. leaf extract-mediated preparation of MgFe2O4 nanoparticles: optical, structural, morphological and particle size analyses. *Solid State Commun*. 2020;2020:114170.
58. Xiang Z, Deng B, Huang C, Liu Z, Song Y, Lu W. Rational design of hollow nanosphere γ-Fe2O3/MWCNTs composites with enhanced electromagnetic wave absorption. *J Alloys Compd*. 2020;822:153570. doi:10.1016/j.jallcom.2019.153570
59. Narvekar AA, Tilve S, Fernandes J. Transformation of a Fe–Mn oxide into a ferromagnetic α-Fe 2 O 3. *J Therm Anal Calorim*. 2019;2019:1–8.
60. Raja S, Vadivel M, Babu RR, Kumar LS, Ramamurthi K. Ferromagnetic and dielectric properties of lead free KNbO3-CoFe2O4 composites. *Solid State Sci*. 2018;85:60–69. doi:10.1016/j.solidstatesciences.2018.09.008
61. Rahmayeni R, Oktavia Y, Stiadi Y, Arief S, Zulhadjri Z. Spinel ferrite of MnFe2O4 synthesized in Piper betle Linn extract media and its application as photocatalysts and antibacterial. *J Dispers Sci Technol*. 2020;2020:1–10.
62. Mohapatra J, Liu JP. Rare-earth-free permanent magnets: the past and future. In: *Handbook of Magnetic Materials*. Elsevier; 2018:1–57.
63. Ansari MO, Ahmad MF, Shadab G, Siddique HR. Superparamagnetic iron oxide nanoparticles based cancer theranostics: a double edge sword to fight against cancer. *J Drug Deliv Sci Technol*. 2018;45:177–183. doi:10.1016/j.jddst.2018.03.017
64. Majetich SA, Wen T, Mefford OT. Magnetic nanoparticles. *MRS Bull*. 2013;38(11):899–903. doi:10.1557/mrs.2013.230
65. Dulińska-Litewka J, Łazarczyk A, Hałubiec P, Szafrański O, Karnas K, Karewicz A. Superparamagnetic iron oxide nanoparticles—current and prospective medical applications. *Materials*. 2019;12(4):617. doi:10.3390/ma12040617
66. Lübbe AS, Bergemann C, Riess H, et al. Clinical experiences with magnetic drug targeting: a Phase I study with 4′-epidoxorubicin in 14 patients with advanced solid tumors. *Cancer Res*. 1996;56(20):4686–4693.
67. Thanh NT, Maclean N, Mahiddine S. Mechanisms of nucleation and growth of nanoparticles in solution. *Chem Rev*. 2014;114(15):7610–7630. doi:10.1021/cr400544s
68. Hernández-Hernández AA, Aguirre-álvarez G, Cariño-Cortés R, Mendoza-Huizar LH, Jiménez-Alvarado R. Iron oxide nanoparticles: synthesis, functionalization, and applications in diagnosis and treatment of cancer. *Chem Pap*. 2020;74:3809–3824. doi:10.1007/s11696-020-01229-8
69. Geonmonond RS, Silva AGD, Camargo PH. Controlled synthesis of noble metal nanomaterials: motivation, principles, and opportunities in nanocatalysis. *An Acad Bras Cienc*. 2018;90(1):719–744. doi:10.1590/0001-3765201820170561
70. Tran H-V, Ngo NM, Medhi R, et al. Multifunctional iron oxide magnetic nanoparticles for biomedical applications: a review. *Materials*. 2022;15(2):503. doi:10.3390/ma15020503
71. Tien NA, Mittova V, Sladkopevtsev B, Mai VQ, Mittova IY, Vuong BX. Structural, optical and magnetic properties of Y-doped NiFe2O4 nanoparticles prepared by simple co-precipitation method. *Solid State Sci*. 2023;138:107149. doi:10.1016/j.solidstatesciences.2023.107149
72. Stolt MJ, Li Z-A, Phillips B, et al. Selective chemical vapor deposition growth of cubic FeGe nanowires that support stabilized magnetic skyrmions. *Nano Lett*. 2017;17(1):508–514. doi:10.1021/acs.nanolett.6b04548
73. Mathur N, Stolt MJ, Niitsu K, et al. Electron holography and magnetotransport measurements reveal stabilized magnetic skyrmions in Fe1–x Co x Si nanowires. *ACS nano*. 2019;13(7):7833–7841. doi:10.1021/acsnano.9b02130
74. Farhanian D, De Crescenzo G, Tavares JR. Large-scale encapsulation of magnetic iron oxide nanoparticles via syngas photo-initiated chemical vapor deposition. *Sci Rep*. 2018;8(1):1–11. doi:10.1038/s41598-018-30802-1
75. Adewunmi AA, Kamal MS, Solling TI. Application of magnetic nanoparticles in demulsification: a review on synthesis, performance, recyclability, and challenges. *J Pet Sci Eng*. 2021;196:107680. doi:10.1016/j.petrol.2020.107680
76. Gorbachev E, Soshnikov M, Wu M, et al. Tuning the particle size, natural ferromagnetic resonance frequency and magnetic properties of ε-Fe 2 O 3 nanoparticles prepared by a rapid sol–gel method. *J Mater Chem C*. 2021;9(19):6173–6179. doi:10.1039/D1TC01242H
77. Kharisov BI, Dias HR, Kharissova OV, Vázquez A, Pena Y, Gomez I. Solubilization, dispersion and stabilization of magnetic nanoparticles in water and non-aqueous solvents: recent trends. *RSC Adv*. 2014;4(85):45354–45381. doi:10.1039/C4RA06902A
78. Xiao W, Su Z, Zhao Y, Wang C. Microwave assisted polyol process for time-saving synthesis of superparamagnetic nanoparticles and application in artificial mimic enzyme. *Nano Express*. 2021;2(2):020001. doi:10.1088/2632-959X/abf2ce
79. Siddiqui M, Nizamuddin S, Baloch HA, et al. Synthesis of magnetic carbon nanocomposites by hydrothermal carbonization and pyrolysis. *Environ Chem Lett*. 2018;16(3):821–844. doi:10.1007/s10311-018-0724-9
80. Yusefi M, Lee-Kiun MS, Shameli K, et al. 5-fluorouracil loaded magnetic cellulose bionanocomposites for potential colorectal cancer treatment. *Carbohydr Polym*. 2021:118523. doi:10.1016/j.carbpol.2021.118523
81. Arteaga-Díaz SJ, Meramo-Hurtado SI, León-Pulido J, Zuorro A, González-Delgado AD. Environmental assessment of large scale production of magnetite (Fe3O4) nanoparticles via coprecipitation. *Appl Sci*. 2019;9(8):1682. doi:10.3390/app9081682
82. Esmaeilkhanian A, Sharifianjazi F, Parvin N, Koti MA. Cytotoxicity of thermoresponsive core/shell NixCo1-xFe2O4/PEG /PEG nanoparticles synthesized by the sol–gel method. *J Phys D*. 2021;54(29):295002. doi:10.1088/1361-6463/abf78a
83. Karoblis D, Zarkov A, Mazeika K, et al. Sol-gel synthesis, structural, morphological and magnetic properties of BaTiO3–BiMnO3 solid solutions. *Ceram Int*. 2020;46(10):16459–16464. doi:10.1016/j.ceramint.2020.03.209
84. Chauhan A, Midha S, Kumar R, et al. Rapid tumor inhibition via magnetic hyperthermia regulated by caspase 3 with time-dependent clearance of iron oxide nanoparticles. *Biomater Sci*. 2021;9(8):2972–2990. doi:10.1039/D0BM01705A
85. Kumar R, Chauhan A, Jha SK, Kuanr BK. Localized cancer treatment by radio-frequency hyperthermia using magnetic nanoparticles immobilized on graphene oxide: from novel synthesis to in vitro studies. *J Mater Chem B*. 2018;6(33):5385–5399. doi:10.1039/C8TB01365A

86. Kumeria T, Maher S, Wang Y, et al. Naturally derived iron oxide nanowires from bacteria for magnetically triggered drug release and cancer hyperthermia in 2D and 3D culture environments: bacteria biofilm to potent cancer therapeutic. *Biomacromolecules*. 2016;17(8):2726–2736. doi:10.1021/acs.biomac.6b00786
87. Shanmugasundaram T, Radhakrishnan M, Poongodi A, Kadirvelu K, Balagurunathan R. Bio-inspired synthesis of superparamagnetic iron oxide nanoparticles for enhanced in vitro anticancer therapy. *MRS Commun*. 2018;8(2):604–609. doi:10.1557/mrc.2018.36
88. Vuong TKO, Le TT, Do HD, et al. PMAO-assisted thermal decomposition synthesis of high-stability ferrofluid based on magnetite nanoparticles for hyperthermia and MRI applications. *Mater Chem Phys*. 2020;245:122762. doi:10.1016/j.matchemphys.2020.122762
89. Asgari M, Soleymani M, Miri T, Barati A. Design of thermosensitive polymer-coated magnetic mesoporous silica nanocomposites with a core-shell-shell structure as a magnetic/temperature dual-responsive drug delivery vehicle. *Polym Adv Technol*. 2021. doi:10.1002/pat.5417
90. Manohar A, Krishnamoorthi C, Pavithra C, Thota N. Magnetic hyperthermia and photocatalytic properties of MnFe 2 O 4 nanoparticles synthesized by solvothermal reflux method. *J Supercond Nov Magn*. 2021;34(1):251–259.
91. Fotukian SM, Barati A, Soleymani M, Alizadeh AM. Solvothermal synthesis of CuFe2O4 and Fe3O4 nanoparticles with high heating efficiency for magnetic hyperthermia application. *J Alloys Compd*. 2020;816:152548. doi:10.1016/j.jallcom.2019.152548
92. Fracasso G, Ghigna P, Nodari L, et al. Nanoaggregates of iron poly-oxo-clusters obtained by laser ablation in aqueous solution of phosphonates. *J Colloid Interface Sci*. 2018;522:208–216. doi:10.1016/j.jcis.2018.03.065
93. Fazio E, Santoro M, Lentini G, Franco D, Guglielmino SPP, Neri F. Iron oxide nanoparticles prepared by laser ablation: synthesis, structural properties and antimicrobial activity. *Colloids Surf a Physicochem Eng Asp*. 2016;490:98–103. doi:10.1016/j.colsurfa.2015.11.034
94. Shaw S, Kailashiya J, Gangwar A, et al. γ-Fe2O3 nanoflowers as efficient magnetic hyperthermia and photothermal agent. *Appl Surf Sci*. 2021:150025. doi:10.1016/j.apsusc.2021.150025
95. Kombaiah K, Vijaya JJ, Kennedy LJ, Bououdina M, Al-Najar B. Conventional and microwave combustion synthesis of optomagnetic CuFe2O4 nanoparticles for hyperthermia studies. *J Phys Chem Solids*. 2018;115:162–171. doi:10.1016/j.jpcs.2017.12.024
96. Salvador M, Gutiérrez G, Noriega S, Moyano A, Blanco-López MC, Matos M. Microemulsion synthesis of superparamagnetic nanoparticles for bioapplications. *Int J Mol Sci*. 2021;22(1):427. doi:10.3390/ijms22010427
97. Nayeem J, Al-Bari MAA, Mahiuddin M, et al. Silica coating of iron oxide magnetic nanoparticles by reverse microemulsion method and their functionalization with cationic polymer P (NIPAm-co-AMPTMA) for antibacterial vancomycin immobilization. *Colloids Surf a Physicochem Eng Asp*. 2021;611:125857. doi:10.1016/j.colsurfa.2020.125857
98. Fuentes-García JsA, Carvalho Alavarse A, Moreno Maldonado AC, Toro-Córdova A, Ibarra MR, Goya, G F., Simple sonochemical method to optimize the heating efficiency of magnetic nanoparticles for magnetic fluid hyperthermia. *ACS omega*. 2020;5(41):26357–26364. doi:10.1021/acsomega.0c02212
99. Dheyab MA, Aziz AA, Jameel MS, Noqta OA, Khaniabadi PM, Mehrdel B. Excellent relaxivity and X-ray attenuation combo properties of Fe3O4@ Au CSNPs produced via rapid sonochemical synthesis for MRI and CT imaging. *Mater Today Commun*. 2020;25:101368. doi:10.1016/j.mtcomm.2020.101368
100. Solzi M, Cugini F, Amade NS, et al. High-temperature magnetic coercivity of CNTs filled with multi-phase Fe-based nanoparticles. *J Magn Magn Mater*. 2020;496:165917. doi:10.1016/j.jmmm.2019.165917
101. Mohammed L, Gomaa HG, Ragab D, Zhu J. Magnetic nanoparticles for environmental and biomedical applications: a review. *Particuology*. 2017;30:1–14. doi:10.1016/j.partic.2016.06.001
102. Jahangirian H, Rafiee-Moghaddam R, Jahangirian N, et al. Green synthesis of zeolite/Fe2O3 nanocomposites: toxicity & cell proliferation assays and application as a smart iron nanofertilizer. *Int J Nanomedicine*. 2020;15:1005. doi:10.2147/IJN.S231679
103. Yew YP, Shameli K, Miyake M, et al. Green biosynthesis of superparamagnetic magnetite Fe3O4 nanoparticles and biomedical applications in targeted anticancer drug delivery system: a review. *Arab J Chem*. 2020;13(1):2287–2308. doi:10.1016/j.arabjc.2018.04.013
104. Izadiyan Z, Shameli K, Miyake M, et al. Cytotoxicity assay of plant-mediated synthesized iron oxide nanoparticles using Juglans regia green husk extract. *Arab J Chem*. 2018;12:2011.
105. Yusefi M, Yee OS, Shameli K. Bio-mediated production and characterisation of magnetic nanoparticles using fruit peel extract. *J Res Nanosci Nanotechnol*. 2021;1(1):53–61. doi:10.37934/jrnn.1.1.5361
106. Jahangirian H, Lemraski EG, Rafiee-Moghaddam R, Webster TJ. A review of using green chemistry methods for biomaterials in tissue engineering. *Int J Nanomedicine*. 2018;13:5953. doi:10.2147/IJN.S163399
107. Gao X, Yokota N, Oda H, Tanaka S, Hokamoto K, Chen P. One step preparation of Fe–FeO–graphene nanocomposite through pulsed wire discharge. *Crystals*. 2018;8(2):104. doi:10.3390/cryst8020104
108. Izadiyan Z, Shameli K, Teow S-Y, et al. Anticancer activity of 5-fluorouracil-loaded nanoemulsions containing Fe3O4/Au core-shell nanoparticles. *J Mol Struct*. 2021:131075. doi:10.1016/j.molstruc.2021.131075
109. Malhotra N, Lee J-S, Liman RAD, et al. Potential toxicity of iron oxide magnetic nanoparticles: a review. *Molecules*. 2020;25(14):3159. doi:10.3390/molecules25143159
110. García A, Espinosa R, Delgado L, et al. Acute toxicity of cerium oxide, titanium oxide and iron oxide nanoparticles using standardized tests. *Desalination*. 2011;269(1–3):136–141. doi:10.1016/j.desal.2010.10.052
111. Mahmoudi M, Hofmann H, Rothen-Rutishauser B, Petri-Fink A. Assessing the in vitro and in vivo toxicity of superparamagnetic iron oxide nanoparticles. *Chem Rev*. 2012;112(4):2323–2338.
112. Mitra S, Nguyen LN, Akter M, Park G, Choi EH, Kaushik NK. Impact of ROS generated by chemical, physical, and plasma techniques on cancer attenuation. *Cancers*. 2019;11(7):1030. doi:10.3390/cancers11071030
113. Markides H, Rotherham M, El Haj A. Biocompatibility and toxicity of magnetic nanoparticles in regenerative medicine. *J Nanomater*. 2012;2012:1–11 doi:10.1155/2012/614094
114. Ran Q, Xiang Y, Liu Y, et al. Eryptosis indices as a novel predictive parameter for biocompatibility of Fe3O4 magnetic nanoparticles on erythrocytes. *Sci Rep*. 2015;5(1):1–15. doi:10.1038/srep16209
115. Ma W, Gehret PM, Hoff RE, Kelly LP, Suh WH. The investigation into the toxic potential of iron oxide nanoparticles utilizing rat pheochromocytoma and human neural stem cells. *Nanomaterials*. 2019;9(3):453. doi:10.3390/nano9030453
116. Marcus M, Karni M, Baranes K, et al. Iron oxide nanoparticles for neuronal cell applications: uptake study and magnetic manipulations. *J Nanobiotechnology*. 2016;14(1):1–12. doi:10.1186/s12951-016-0190-0

117. Spiridonov V, Panova I, Makarova L, et al. The one-step synthesis of polymer-based magnetic γ-Fe2O3/carboxymethyl cellulose nanocomposites. *Carbohydr Polym*. 2017;177:269–274. doi:10.1016/j.carbpol.2017.08.126
118. Arami H, Khandhar A, Liggitt D, Krishnan KM. In vivo delivery, pharmacokinetics, biodistribution and toxicity of iron oxide nanoparticles. *Chem Soc Rev*. 2015;44(23):8576–8607. doi:10.1039/c5cs00541h
119. Wada S, Yue L, Tazawa K, et al. New local hyperthermia using dextran magnetite complex (DM) for oral cavity: experimental study in normal hamster tongue. *Oral Dis*. 2001;7(3):192–195. doi:10.1034/j.1601-0825.2001.70309.x
120. Frericks BB, Wacker F, Loddenkemper C, et al. Magnetic resonance imaging of experimental inflammatory bowel disease: quantitative and qualitative analyses with histopathologic correlation in a rat model using the ultrasmall iron oxide SHU 555 C. *Invest Radiol*. 2009;44(1):23–30. doi:10.1097/RLI.0b013e3181899025
121. Bourrinet P, Bengele HH, Bonnemain B, et al. Preclinical safety and pharmacokinetic profile of ferumoxtran-10, an ultrasmall superparamagnetic iron oxide magnetic resonance contrast agent. *Invest Radiol*. 2006;41(3):313–324. doi:10.1097/01.rli.0000197669.80475.dd
122. Aslani R, Namazi H. Fabrication of a new photoluminescent and pH-responsive nanocomposite based on a hyperbranched polymer prepared from amino acid for targeted drug delivery applications. *Int J Pharm*. 2023;636:122804. doi:10.1016/j.ijpharm.2023.122804
123. Bhattacharya S, Prajapati BG, Singh S. A critical review on the dissemination of pH and stimuli-responsive polymeric nanoparticular systems to improve drug delivery in cancer therapy. *Crit Rev Oncol Hematol*. 2023;185:103961. doi:10.1016/j.critrevonc.2023.103961
124. Hoogenboom R. Temperature-responsive polymers: properties, synthesis, and applications. In: *Smart Polymers and Their Applications*. Elsevier; 2019:13–44.
125. Yew YP, Shameli K, Mohamad SEB, et al. Potential anticancer activity of protocatechuic acid loaded in montmorillonite/Fe3O4 nanocomposites stabilized by seaweed Kappaphycus alvarezii. *Int J Pharm*. 2019;572:118743. doi:10.1016/j.ijpharm.2019.118743
126. Yusefi M, Shameli K, Chan Zhe J, Bin Che Sidik NA. Preparation and characterization of cross-linked chitosan/cellulose bionanohybrids. Paper presented at: International Conference on Mechanical Engineering Research; 2023.
127. Kaur N, Gupta AK. Applications of inulin and oligofructose in health and nutrition. *J Biosci*. 2002;27(7):703–714. doi:10.1007/BF02708379
128. Souza LO, Lessa OA, Dias MC, et al. Study of morphological properties and rheological parameters of cellulose nanofibrils of cocoa shell (Theobroma cacao L.). *Carbohydr Polym*. 2019;214:152–158. doi:10.1016/j.carbpol.2019.03.037
129. Wijaya CJ, Ismadji S, Gunawan S. A review of lignocellulosic-derived nanoparticles for drug delivery applications: lignin nanoparticles, xylan nanoparticles, and cellulose nanocrystals. *Molecules*. 2021;26(3):676. doi:10.3390/molecules26030676
130. Long W, Ouyang H, Zhou C, et al. Simultaneous surface functionalization and drug loading: a novel method for fabrication of cellulose nanocrystals-based pH responsive drug delivery system. *Int J Biol Macromol*. 2021;182:2066–2075. doi:10.1016/j.ijbiomac.2021.05.193
131. Low LE, Tan LT-H, Goh B-H, Tey BT, Ong BH, Tang SY. Magnetic cellulose nanocrystal stabilized pickering emulsions for enhanced bioactive release and human colon cancer therapy. *Int J Biol Macromol*. 2019;127:76–84. doi:10.1016/j.ijbiomac.2019.01.037
132. Ntoutoume GMN, Granet R, Mbakidi JP, et al. Development of curcumin–cyclodextrin/cellulose nanocrystals complexes: new anticancer drug delivery systems. *Bioorg Med Chem Lett*. 2016;26(3):941–945. doi:10.1016/j.bmcl.2015.12.060
133. Iurciuc-Tincu C-E, Cretan MS, Purcar V, et al. Drug delivery system based on pH-sensitive biocompatible poly (2-vinyl pyridine)-b-poly (ethylene oxide) nanomicelles loaded with curcumin and 5-fluorouracil. *Polymers*. 2020;12(7):1450. doi:10.3390/polym12071450
134. He T, Wang W, Chen B, Wang J, Liang Q, Chen B. 5-Fluorouracil monodispersed chitosan microspheres: microfluidic chip fabrication with crosslinking, characterization, drug release and anticancer activity. *Carbohydr Polym*. 2020;236:116094. doi:10.1016/j.carbpol.2020.116094
135. Parhi R. Drug delivery applications of chitin and chitosan: a review. *Environ Chem Lett*. 2020;18(3):577–594. doi:10.1007/s10311-020-00963-5
136. Wang F, Zhang Q, Huang K, et al. Preparation and characterization of carboxymethyl cellulose containing quaternized chitosan for potential drug carrier. *Int J Biol Macromol*. 2020;154:1392–1399. doi:10.1016/j.ijbiomac.2019.11.019
137. Mohan D, Khairullah NF, How YP, Sajab MS, Kaco H. 3D printed laminated CaCO3-nanocellulose films as controlled-release 5-fluorouracil. *Polymers*. 2020;12(4):986. doi:10.3390/polym12040986
138. Yusefi M, Shameli K, Jahangirian H, et al. The potential anticancer activity of 5-fluorouracil loaded in cellulose fibers isolated from rice straw. *Int J Nanomedicine*. 2020;15:5417. doi:10.2147/IJN.S250047
139. Mariadoss AVA, Saravanakumar K, Sathiyaseelan A, Venkatachalam K, Wang M-H. Folic acid functionalized starch encapsulated green synthesized copper oxide nanoparticles for targeted drug delivery in breast cancer therapy. *Int J Biol Macromol*. 2020;164:2073–2084. doi:10.1016/j.ijbiomac.2020.08.036
140. Mishra A, Pandey VK, Shankar BS, Melo JS. Spray drying as an efficient route for synthesis of silica nanoparticles-sodium alginate biohybrid drug carrier of doxorubicin. *Colloids Surf B Biointerfaces*. 2021;197:111445. doi:10.1016/j.colsurfb.2020.111445
141. El-Emam SZ, El-Ella DMA, Fayez SM, Asker M, Nazeam JA. Novel dandelion mannan-lipid nanoparticle: exploring the molecular mechanism underlying the potent anticancer effect against non-small lung carcinoma. *J Funct Foods*. 2021;87:104781. doi:10.1016/j.jff.2021.104781
142. Huang G, Huang H. Hyaluronic acid-based biopharmaceutical delivery and tumor-targeted drug delivery system. *J Control Release*. 2018;278:122–126. doi:10.1016/j.jconrel.2018.04.015
143. Li Q, Ye L, Zhang A, Feng Z. The preparation and morphology control of heparin-based pH sensitive polyion complexes and their application as drug carriers. *Carbohydr Polym*. 2019;211:370–379. doi:10.1016/j.carbpol.2019.01.089
144. Singh RS, Kaur N, Hassan M, Kennedy JF. Pullulan in biomedical research and development-A review. *Int J Biol Macromol*. 2021;166:694–706. doi:10.1016/j.ijbiomac.2020.10.227
145. Mutlu EC, Bahadori F, Bostan MS, Sarilmiser HK, ToksoyOner E, Eroğlu MS. Halomonas Levan-coated phospholipid based nano-carrier for active targeting of A549 lung cancer cells. *Eur Polym J*. 2021;144:110239. doi:10.1016/j.eurpolymj.2020.110239
146. Ullah MW, Ul-Islam M, Khan T, Park JK. Recent developments in the synthesis, properties, and applications of various microbial polysaccharides. In: *Handbook of Hydrocolloids*. Elsevier; 2021:975–1015.
147. Villarreal-Otalvaro C, Coburn JM. Fabrication methods and form factors of gellan gum-based materials for drug delivery and anti-cancer applications. *ACS Biomater Sci Eng*. 2021. doi:10.1021/acsbiomaterials.1c00685
148. Wang X, Qi Y, Liu L, Ganbold T, Baigude H, Han J. Preparation and cell activities of lactosylated curdlan-triornithine nanoparticles for enhanced DNA/siRNA delivery in hepatoma cells. *Carbohydr Polym*. 2019;225:115252. doi:10.1016/j.carbpol.2019.115252
149. Kim Y, Hu Y, Jeong J-p, Jung S. Injectable, self-healable and adhesive hydrogels using oxidized Succinoglycan/chitosan for pH-responsive drug delivery. *Carbohydr Polym*. 2022;284119195. doi:10.1016/j.carbpol.2022.119195

150. Soh H-S, Kim C-S, Lee S-P. A new in vitro assay of cholesterol adsorption by food and microbial polysaccharides. *J Med Food*. 2003;6(3):225–230. doi:10.1089/10966200360716643
151. Djekic L, Ćirić A. Micro-and nanoscale drug delivery systems based on xanthan gum hydrogels. In: *Micro-and Nanoengineered Gum-Based Biomaterials for Drug Delivery and Biomedical Applications*. Elsevier; 2022:35–76.
152. Naseri N, Iranshahi M, Tayarani-Najaran Z, Rakhshani S, Mohtashami L. Enhanced cytotoxicity of auraptene to prostate cancer cells by dextran-coated Fe3O4 nanoparticles. *Nanomed J*. 2022;9(1):77–86.
153. Oh Y, Lee N, Kang HW, Oh J. In vitro study on apoptotic cell death by effective magnetic hyperthermia with chitosan-coated MnFe2O4. *Nanotechnology*. 2016;27(11):115101. doi:10.1088/0957-4484/27/11/115101
154. Soleymani M, Khalighfard S, Khodayari S, et al. Effects of multiple injections on the efficacy and cytotoxicity of folate-targeted magnetite nanoparticles as theranostic agents for MRI detection and magnetic hyperthermia therapy of tumor cells. *Sci Rep*. 2020;10(1):1–14. doi:10.1038/s41598-020-58605-3
155. Iqbal Y, Bae H, Rhee I, Hong S. Control of the saturation temperature in magnetic heating by using polyethylene-glycol-coated rod-shaped nickel-ferrite (NiFe 2 O 4) nanoparticles. *J Korean Phys Soc*. 2016;68(4):587–592. doi:10.3938/jkps.68.587
156. Lahiri B, Muthukumaran T, Philip J. Magnetic hyperthermia in phosphate coated iron oxide nanofluids. *J Magn Magn Mater*. 2016;407:101–113. doi:10.1016/j.jmmm.2016.01.044
157. Iqbal Y, Bae H, Rhee I, Hong S. Magnetic heating of silica-coated manganese ferrite nanoparticles. *J Magn Magn Mater*. 2016;409:80–86. doi:10.1016/j.jmmm.2016.02.078
158. Hanini A, Lartigue L, Gavard J, et al. Zinc substituted ferrite nanoparticles with Zn0. 9Fe2. 1O4 formula used as heating agents for in vitro hyperthermia assay on glioma cells. *J Magn Magn Mater*. 2016;416:315–320. doi:10.1016/j.jmmm.2016.05.016
159. Gupta R, Sharma D. Biofunctionalization of magnetite nanoparticles with stevioside: effect on the size and thermal behaviour for use in hyperthermia applications. *Int J Hyperthermia*. 2019. doi:10.1080/02656736.2019.1565787
160. Gupta R, Sharma D. Manganese-doped magnetic nanoclusters for hyperthermia and photothermal glioblastoma therapy. *ACS Appl Nano Mater*. 2020;3(2):2026–2037. doi:10.1021/acsanm.0c00121
161. Rego GN, Nucci MP, Mamani JB, et al. Therapeutic efficiency of multiple applications of magnetic hyperthermia technique in glioblastoma using aminosilane coated iron oxide nanoparticles: in vitro and in vivo study. *Int J Mol Sci*. 2020;21(3):958. doi:10.3390/ijms21030958
162. Patil R, Thorat N, Shete P, Otari S, Tiwale B, Pawar S. In vitro hyperthermia with improved colloidal stability and enhanced SAR of magnetic core/shell nanostructures. *Mater Sci Eng C*. 2016;59:702–709.
163. Iacob M, Racles C, Dascalu MC, Tugui C, Lozan V, Cazacu M. Nanomaterials developed by processing iron coordination compounds for biomedical application. *J Nanomater*. 2019;2019:1–4.
164. Agotegaray MA, Lassalle VL. *Silica-Coated Magnetic Nanoparticles: An Insight into Targeted Drug Delivery and Toxicology*. Springer; 2017.
165. Pawar S, Takke A. Regulatory aspects, types, and bioapplications of metallic nanoparticles: a review. *Curr Drug Deliv*. 2023:20(7);857–883. doi:10.2174/1567201819666220817110025
166. Adam A, Harlepp S, Ghilini F, et al. Core-shell iron oxide@ stellate mesoporous silica for combined near-infrared photothermia and drug delivery: influence of pH and surface chemistry. *Colloids Surf Physicochem Eng Asp*. 2022;640:128407. doi:10.1016/j.colsurfa.2022.128407
167. Horny M-C, Gamby J, Dupuis V, Siaugue J-M. Magnetic hyperthermia on γ-Fe2O3@ SiO2 core-shell nanoparticles for mi-RNA 122 detection. *Nanomaterials*. 2021;11(1):149. doi:10.3390/nano11010149
168. Tian H, Zhang R, Li J, et al. A novel yolk–shell Fe3O4@ mesoporous carbon nanoparticle as an effective tumor-targeting nanocarrier for improvement of chemotherapy and photothermal therapy. *Int J Mol Sci*. 2022;23(3):1623. doi:10.3390/ijms23031623
169. Taherkhani A, Fazli H, Taherkhani F. Application of janus magnetic nanoparticle Fe3O4@ SiN functionalized with beta-cyclodextrin in thymol drug delivery procedure: an in vitro study. *Appl Organomet Chem*. 2021;35(11):e6399. doi:10.1002/aoc.6399
170. Hou S, Mahadevegowda SH, Lu D, Zhang K, Chan-Park MB, Duan H. Metabolic labeling mediated targeting and thermal killing of gram-positive bacteria by self-reporting janus magnetic nanoparticles. *Small*. 2021;17(2):2006357. doi:10.1002/smll.202006357
171. Hepel M. Magnetic nanoparticles for nanomedicine. *Magnetochemistry*. 2020;6(1):3. doi:10.3390/magnetochemistry6010003
172. Wulandari IO, Mardila VT, Santjojo DDH, Sabarudin A. Preparation and characterization of chitosan-coated Fe3O4 nanoparticles using ex-situ co-precipitation method and tripolyphosphate/sulphate as dual crosslinkers. Paper presented at: IOP Conference Series: Materials Science and Engineering; 2018.
173. Jiang L, Chai F, Chen Q. Soft magnetic nanocomposite microgels by in-situ crosslinking of poly acrylic acid onto superparamagnetic magnetite nanoparticles and their applications for the removal of Pb (II) ion. *Eur Polym J*. 2017;89:468–481. doi:10.1016/j.eurpolymj.2017.02.045
174. Su H, Han X, He L, et al. Synthesis and characterization of magnetic dextran nanogel doped with iron oxide nanoparticles as magnetic resonance imaging probe. *Int J Biol Macromol*. 2019;128:768–774. doi:10.1016/j.ijbiomac.2019.01.219
175. Malhotra N, Audira G, Chen J-R, et al. Surface modification of magnetic nanoparticles by carbon-coating can increase its biosafety: evidences from biochemical and neurobehavioral tests in zebrafish. *Molecules*. 2020;25(9):2256. doi:10.3390/molecules25092256
176. Wang D, Li X, Li X, et al. Magnetic and pH dual-responsive nanoparticles for synergistic drug-resistant breast cancer chemo/photodynamic therapy. *Int J Nanomedicine*. 2019;14:7665. doi:10.2147/IJN.S214377
177. Lee N, Yoo D, Ling D, Cho MH, Hyeon T, Cheon J. Iron oxide based nanoparticles for multimodal imaging and magnetoresponsive therapy. *Chem Rev*. 2015;115(19):10637–10689.
178. Giustini AJ, Petryk AA, Cassim SM, Tate JA, Baker I, Hoopes PJ. Magnetic nanoparticle hyperthermia in cancer treatment. *Nano Life*. 2010;1(01n02):17–32. doi:10.1142/S1793984410000067
179. Willis AJ, Pernal SP, Gaertner ZA, et al. Rotating magnetic nanoparticle clusters as microdevices for drug delivery. *Int J Nanomedicine*. 2020;15:4105. doi:10.2147/IJN.S247985
180. Obaidat IM, Narayanaswamy V, Alaabed S, Sambasivam S, Muralee Gopi CV. Principles of magnetic hyperthermia: a focus on using multifunctional hybrid magnetic nanoparticles. *Magnetochemistry*. 2019;5(4):67. doi:10.3390/magnetochemistry5040067
181. Wildeboer R, Southern P, Pankhurst Q. On the reliable measurement of specific absorption rates and intrinsic loss parameters in magnetic hyperthermia materials. *J Phys D: Appl Phys*. 2014;47(49):495003.
182. Wang S-Y, Huang S, Borca-Tasciuc D-A. Potential sources of errors in measuring and evaluating the specific loss power of magnetic nanoparticles in an alternating magnetic field. *IEEE Trans Magn*. 2012;49(1):255–262. doi:10.1109/TMAG.2012.2224648

183. Dadfar SM, Camozzi D, Darguzyte M, et al. Size-isolation of superparamagnetic iron oxide nanoparticles improves MRI, MPI and hyperthermia performance. *J Nanobiotechnology*. 2020;18(1):1–13. doi:10.1186/s12951-020-0580-1
184. Fopase R, Saxena V, Seal P, Borah J, Pandey LM. Yttrium iron garnet for hyperthermia applications: synthesis, characterization and in-vitro analysis. *Mater Sci Eng C*. 2020;116:111163. doi:10.1016/j.msec.2020.111163
185. Crezee J, Franken NA, Oei AL. Hyperthermia-based anti-cancer treatments. *Cancers*. 2021;13:1240
186. Behrouzkia Z, Joveini Z, Keshavarzi B, Eyvazzadeh N, Aghdam RZ. Hyperthermia: how can it be used? *Oman Med J*. 2016;31(2):89. doi:10.5001/omj.2016.19
187. Moise S, Byrne JM, El Haj AJ, Telling ND. The potential of magnetic hyperthermia for triggering the differentiation of cancer cells. *Nanoscale*. 2018;10(44):20519–20525. doi:10.1039/C8NR05946B
188. Nguyen LH, Phong PT, Nam PH, et al. The role of anisotropy in distinguishing domination of Néel or Brownian relaxation contribution to magnetic inductive heating: orientations for biomedical applications. *Materials*. 2021;14(8):1875. doi:10.3390/ma14081875
189. Nikitin AA, Ivanova AV, Semkina AS, Lazareva PA, Abakumov MA. Magneto-mechanical approach in biomedicine: benefits, challenges, and future perspectives. *Int J Mol Sci*. 2022;23(19):11134. doi:10.3390/ijms231911134
190. Maluta S, Kolff MW. Role of hyperthermia in breast cancer locoregional recurrence: a review. *Breast Care*. 2015;10(6):408–412. doi:10.1159/000440792
191. Niculaes D, Lak A, Anyfantis GC, et al. Asymmetric assembling of iron oxide nanocubes for improving magnetic hyperthermia performance. *ACS nano*. 2017;11(12):12121–12133. doi:10.1021/acsnano.7b05182
192. Sugumaran PJ, Liu X-L, Herng TS, Peng E, Ding J. GO-functionalized large magnetic iron oxide nanoparticles with enhanced colloidal stability and hyperthermia performance. *ACS Appl Mater Interfaces*. 2019;11(25):22703–22713. doi:10.1021/acsami.9b04261
193. Salunkhe AB, Khot VM, Ruso JM, Patil S. Water dispersible superparamagnetic Cobalt iron oxide nanoparticles for magnetic fluid hyperthermia. *J Magn Magn Mater*. 2016;419:533–542. doi:10.1016/j.jmmm.2016.06.057
194. Hajalilou A, Ferreira L, Jorge M, Reis C, Cruz M. Superparamagnetic Ag-Fe3O4 composites nanoparticles for magnetic fluid hyperthermia. *J Magn Magn Mater*. 2021:168242. doi:10.1016/j.jmmm.2021.168242
195. Umut E, Coşkun M, Pineider F, Berti D, Güngüneş H. Nickel ferrite nanoparticles for simultaneous use in magnetic resonance imaging and magnetic fluid hyperthermia. *J Colloid Interface Sci*. 2019;550:199–209. doi:10.1016/j.jcis.2019.04.092
196. Nayek C, Manna K, Bhattacharjee G, Murugavel P, Obaidat I. Investigating size-and temperature-dependent coercivity and saturation magnetization in PEG coated Fe3O4 nanoparticles. *Magnetochemistry*. 2017;3(2):19. doi:10.3390/magnetochemistry3020019
197. Munjal S, Khare N, Sivakumar B, Sakthikumar DN. Citric acid coated CoFe2O4 nanoparticles transformed through rapid mechanochemical ligand exchange for efficient magnetic hyperthermia applications. *J Magn Magn Mater*. 2019;477:388–395. doi:10.1016/j.jmmm.2018.09.007
198. He S, Zhang H, Liu Y, et al. Maximizing specific loss power for magnetic hyperthermia by hard–soft mixed ferrites. *Small*. 2018;14(29):1800135. doi:10.1002/smll.201800135
199. Rajan A, Sharma M, Sahu NK. Assessing magnetic and inductive thermal properties of various surfactants functionalised Fe 3 O 4 nanoparticles for hyperthermia. *Sci Rep*. 2020;10(1):1–15. doi:10.1038/s41598-020-71703-6
200. Jasso-Terán RA, Cortés-Hernández DA, Sánchez-Fuentes HJ, et al. Synthesis, characterization and hemolysis studies of Zn (1− x) CaxFe2O4 ferrites synthesized by sol-gel for hyperthermia treatment applications. *J Magn Magn Mater*. 2017;427:241–244. doi:10.1016/j.jmmm.2016.10.099
201. Lachowicz D, Górka W, Kmita A, et al. Enhanced hyperthermic properties of biocompatible zinc ferrite nanoparticles with a charged polysaccharide coating. *J Mater Chem B*. 2019;7(18):2962–2973. doi:10.1039/C9TB00029A
202. Hirosawa F, Iwasaki T, Watano S. Synthesis and magnetic induction heating properties of Gd-substituted Mg–Zn ferrite nanoparticles. *Appl Nanosci*. 2017;7(5):209–214. doi:10.1007/s13204-017-0566-y
203. Yusefi M, Shameli K, Ali RR, Pang S-W, Teow S-Y. Evaluating anticancer activity of plant-mediated synthesized iron oxide nanoparticles using Punica granatum fruit peel extract. *J Mol Struct*. 2020;1204:127539. doi:10.1016/j.molstruc.2019.127539
204. Wang Y-J, Lin P-Y, Hsieh S-L, et al. Utilizing edible agar as a carrier for dual functional doxorubicin-Fe3O4 nanotherapy drugs. *Materials*. 2021;14(8):1824. doi:10.3390/ma14081824
205. Lachowicz D, Kaczyńska A, Wirecka R, et al. A hybrid system for magnetic hyperthermia and drug delivery: SPION functionalized by curcumin conjugate. *Materials*. 2018;11(12):2388. doi:10.3390/ma11122388
206. Galli M, Guerrini A, Cauteruccio S, et al. Superparamagnetic iron oxide nanoparticles functionalized by peptide nucleic acids. *RSC Adv*. 2017;7(25):15500–15512. doi:10.1039/C7RA00519A
207. Oh Y, Moorthy MS, Manivasagan P, Bharathiraja S, Oh J. Magnetic hyperthermia and pH-responsive effective drug delivery to the sub-cellular level of human breast cancer cells by modified CoFe2O4 nanoparticles. *Biochimie*. 2017;133:7–19. doi:10.1016/j.biochi.2016.11.012
208. Zamora-Mora V, Fernández-Gutiérrez M, González-Gómez Á, et al. Chitosan nanoparticles for combined drug delivery and magnetic hyperthermia: from preparation to in vitro studies. *Carbohydr Polym*. 2017;157:361–370. doi:10.1016/j.carbpol.2016.09.084
209. Ferjaoui Z, Jamal Al Dine E, Kulmukhamedova A, et al. Doxorubicin-loaded thermoresponsive superparamagnetic nanocarriers for controlled drug delivery and magnetic hyperthermia applications. *ACS Appl Mater Interfaces*. 2019;11(34):30610–30620. doi:10.1021/acsami.9b10444
210. Yao X, Niu X, Ma K, et al. Graphene quantum dots-capped magnetic mesoporous silica nanoparticles as a multifunctional platform for controlled drug delivery, magnetic hyperthermia, and photothermal therapy. *Small*. 2017;13(2):1602225. doi:10.1002/smll.201602225
211. Jabalera Y, Oltolina F, Peigneux A, et al. Nanoformulation design including MamC-mediated biomimetic nanoparticles allows the simultaneous application of targeted drug delivery and magnetic hyperthermia. *Polymers*. 2020;12(8):1832. doi:10.3390/polym12081832
212. Xue W, Liu X-L, Ma H, et al. AMF responsive DOX-loaded magnetic microspheres: transmembrane drug release mechanism and multi-modality postsurgical treatment of breast cancer. *J Mater Chem B*. 2018;6(15):2289–2303. doi:10.1039/C7TB03206D
213. Kurian J, Lahiri B, Mathew MJ, Philip J. High magnetic fluid hyperthermia efficiency in copper ferrite nanoparticles prepared by solvothermal and hydrothermal methods. *J Magn Magn Mater*. 2021:168233. doi:10.1016/j.jmmm.2021.168233
214. Phong P, Nam P, Manh D, Lee I-J. Mn0. 5Zn0. 5Fe2O4 nanoparticles with high intrinsic loss power for hyperthermia therapy. *J Magn Magn Mater*. 2017;433:76–83. doi:10.1016/j.jmmm.2017.03.001
215. El-Sayed H, Ali I, Azzam A, Sattar A. Influence of the magnetic dead layer thickness of Mg-Zn ferrites nanoparticle on their magnetic properties. *J Magn Magn Mater*. 2017;424:226–232. doi:10.1016/j.jmmm.2016.10.049

216. Chen R, Christiansen MG, Sourakov A, et al. High-performance ferrite nanoparticles through nonaqueous redox phase tuning. *Nano Lett*. 2016;16(2):1345–1351. doi:10.1021/acs.nanolett.5b04761
217. Reyes-Ortega F, Delgado ÁV, Schneider EK, Checa Fernández B, Iglesias GR. Magnetic nanoparticles coated with a thermosensitive polymer with hyperthermia properties. *Polymers*. 2018;10(1):10. doi:10.3390/polym10010010
218. Das R, Alonso J, Nemati Porshokouh Z, et al. Tunable high aspect ratio iron oxide nanorods for enhanced hyperthermia. *J Phys Chem C*. 2016;120(18):10086–10093. doi:10.1021/acs.jpcc.6b02006
219. Sasikala ARK, Thomas RG, Unnithan AR, et al. Multifunctional nanocarpets for cancer theranostics: remotely controlled graphene nanoheaters for thermo-chemosensitisation and magnetic resonance imaging. *Sci Rep*. 2016;6(1):1–14.
220. Thirunavukkarasu GK, Cherukula K, Lee H, Jeong YY, Park I-K, Lee JY. Magnetic field-inducible drug-eluting nanoparticles for image-guided thermo-chemotherapy. *Biomaterials*. 2018;180:240–252. doi:10.1016/j.biomaterials.2018.07.028
221. Rajan A, Kaczmarek-Szczepańskac B, Sahu NK. Magneto-thermal response of Fe3O4@ CTAB nanoparticles for cancer hyperthermia applications. *Mater Today Commun*. 2021;28:102583. doi:10.1016/j.mtcomm.2021.102583
222. Ognjanović M, Stanković DM, Jaćimović ŽK, Kosović-Perutović M, Dojčinović B, Antić B. The effect of surface-modifier of magnetite nanoparticles on electrochemical detection of dopamine and heating efficiency in magnetic hyperthermia. *J Alloys Compd*. 2021:161075. doi:10.1016/j.jallcom.2021.161075
223. Fuller EG, Sun H, Dhavalikar RD, et al. Externally triggered heat and drug release from magnetically controlled nanocarriers. *ACS Appl Polym Mater*. 2019;1(2):211–220. doi:10.1021/acsapm.8b00100
224. Nemati Z, Alonso J, Rodrigo I, et al. Improving the heating efficiency of iron oxide nanoparticles by tuning their shape and size. *J Phys Chem C*. 2018;122(4):2367–2381. doi:10.1021/acs.jpcc.7b10528
225. Jaidev L, Chellappan DR, Bhavsar DV, et al. Multi-functional nanoparticles as theranostic agents for the treatment & imaging of pancreatic cancer. *Acta Biomater*. 2017;49:422–433. doi:10.1016/j.actbio.2016.11.053
226. Beola L, Grazú V, Fernández-Afonso Y, et al. Critical parameters to improve pancreatic cancer treatment using magnetic hyperthermia: field conditions, immune response, and particle biodistribution. *ACS Appl Mater Interfaces*. 2021;13(11):12982–12996. doi:10.1021/acsami.1c02338
227. Tong S, Quinto CA, Zhang L, Mohindra P, Bao G. Size-dependent heating of magnetic iron oxide nanoparticles. *Acs Nano*. 2017;11 (7):6808–6816. doi:10.1021/acsnano.7b01762
228. Chauhan A, Kumar R, Singh P, Jha SK, Kuanr BK. RF hyperthermia by encapsulated Fe3O4 nanoparticles induces cancer cell death via time-dependent caspase-3 activation. *Nanomedicine*. 2020;15(04):355–379. doi:10.2217/nnm-2019-0187
229. Kumar R, Chauhan A, Jha SK, Kuanr BK. Encapsulated lanthanum strontium manganese oxide in mesoporous silica shell: potential for cancer treatment by hyperthermia therapy. *J Alloys Compd*. 2019;790:433–446. doi:10.1016/j.jallcom.2019.03.163
230. Pon-On W, Tithito T, Maneeprakorn W, Phenrat T, Tang I-M. Investigation of magnetic silica with thermoresponsive chitosan coating for drug controlled release and magnetic hyperthermia application. *Mater Sci Eng C*. 2019;97:23–30. doi:10.1016/j.msec.2018.11.076
231. Kandasamy G, Sudame A, Bhati P, Chakrabarty A, Maity D. Systematic investigations on heating effects of carboxyl-amine functionalized superparamagnetic iron oxide nanoparticles (SPIONs) based ferrofluids for in vitro cancer hyperthermia therapy. *J Mol Liq*. 2018;256:224–237. doi:10.1016/j.molliq.2018.02.029
232. Kumar R, Chauhan A, Kuanr BK. A robust in vitro anticancer activity via magnetic hyperthermia mediated by colloidally stabilized mesoporous silica encapsulated La0. 7Sr0. 3MnO3 core-shell structure. *Colloids Surf Physicochem Eng Asp*. 2021;615:126212. doi:10.1016/j.colsurfa.2021.126212
233. Nieciecka D, Celej J, Żuk M, et al. Hybrid system for local drug delivery and magnetic hyperthermia based on SPIONs loaded with doxorubicin and epirubicin. *Pharmaceutics*. 2021;13(4):480. doi:10.3390/pharmaceutics13040480
234. Sánchez J, Rodríguez-Reyes M, Cortés-Hernández DA, Ávila-Orta CA, Reyes-Rodríguez PY. Heating capacity and biocompatibility of pluronic-coated manganese gallium ferrites for magnetic hyperthermia treatment. *Colloids Surf Physicochem Eng Asp*. 2021;612:125986. doi:10.1016/j.colsurfa.2020.125986
235. Hedayatnasab Z, Dabbagh A, Abnisa F, Daud WMAW. Polycaprolactone-coated superparamagnetic iron oxide nanoparticles for in vitro magnetic hyperthermia therapy of cancer. *Eur Polym J*. 2020;133:109789.
236. Ramirez-Nuñez A, Jimenez-Garcia L, Goya G, Sanz B, Santoyo-Salazar J. In vitro magnetic hyperthermia using polyphenol-coated Fe3O4@ γFe2O3 nanoparticles from Cinnamomun verum and Vanilla planifolia: the concert of green synthesis and therapeutic possibilities. *Nanotechnology*. 2018;29(7):074001. doi:10.1088/1361-6528/aaa2c1
237. Minaei SE, Khoei S, Khoee S, Vafashoar F, Mahabadi VP. In vitro anti-cancer efficacy of multi-functionalized magnetite nanoparticles combining alternating magnetic hyperthermia in glioblastoma cancer cells. *Mater Sci Eng C*. 2019;101:575–587. doi:10.1016/j.msec.2019.04.007
238. Wang C, Hsu C-H, Li Z, et al. Effective heating of magnetic nanoparticle aggregates for in vivo nano-theranostic hyperthermia. *Int J Nanomedicine*. 2017;12:6273. doi:10.2147/IJN.S141072
239. Deb PK, Al-Jaidi B, Akkinepalli RR, Al-Aboudi A, Tekade RK. Biomaterials and nanoparticles for hyperthermia therapy. In: *Biomaterials and Bionanotechnology*. Elsevier; 2019:375–413.
240. Chang M, Hou Z, Wang M, Li C, Lin J. Recent advances in hyperthermia therapy-based synergistic immunotherapy. *Adv Mater*. 2021;33 (4):2004788. doi:10.1002/adma.202004788
241. Takeda T, Takeda H, Tanaka C, Maruhashi S. The effect of immunotherapy and hyperthermia for advanced or recurrent head and neck cancer-74 clinical cases. *Gan To Kagaku Ryoho*. 2014;41(10):1283–1285.
242. Jha S, Sharma PK, Malviya R. Hyperthermia: role and risk factor for cancer treatment. *Achiev Life Sci*. 2016;10(2):161–167. doi:10.1016/j.als.2016.11.004
243. Mallory M, Gogineni E, Jones GC, Greer L, Simone II CB. Therapeutic hyperthermia: the old, the new, and the upcoming. *Crit Rev Oncol*. 2016;97:56–64. doi:10.1016/j.critrevonc.2015.08.003
244. Heckel-Reusser S. Whole-Body Hyperthermia (WBH): historical aspects, current use, and future perspectives. In: *Water-Filtered Infrared a (Wira) Irradiation*. Springer, Cham; 2022:143–154.
245. Wust P, Hildebrandt B, Sreenivasa G, et al. Hyperthermia in combined treatment of cancer. *Lancet Oncol*. 2002;3(8):487–497. doi:10.1016/S1470-2045(02)00818-5

246. Atmaca A, Al-Batran S-E, Neumann A, et al. Whole-body hyperthermia (WBH) in combination with carboplatin in patients with recurrent ovarian cancer—A Phase II study. *Gynecol Oncol*. 2009;112(2):384–388. doi:10.1016/j.ygyno.2008.11.001
247. Jia D, Liu J. Current devices for high-performance whole-body hyperthermia therapy. *Expert Rev Med Devices*. 2010;7(3):407–423. doi:10.1586/erd.10.13
248. Van Rhoon G, Franckena M, Ten Hagen T. A moderate thermal dose is sufficient for effective free and TSL based thermochemotherapy. *Adv Drug Deliv Rev*. 2020;163:145–156. doi:10.1016/j.addr.2020.03.006
249. Schouten D, van Os R, Westermann AM, et al. A randomized phase-II study of reirradiation and hyperthermia versus reirradiation and hyperthermia plus chemotherapy for locally recurrent breast cancer in previously irradiated area. *Acta Oncol*. 2022;61(4):441–448. doi:10.1080/0284186X.2022.2033315
250. Conte E, Psihogios A, Seely D. Hyperthermia in cancer care: a literature review. *CAND J*. 2021;28(3):14–30. doi:10.54434/candj.92
251. Tyagi P, Bajpai K, Dwivedi R, Sharma N, Mudgal P. Patch antenna for microwave hyperthermia applications. Proceedings of the Advancement in Electronics & Communication Engineering (July 14, 2022); 2022.
252. Boutros C, Somasundar P, Espat NJ. Early results on the use of biomaterials as adjuvant to abdominal wall closure following cytoreduction and hyperthermic intraperitoneal chemotherapy. *World J Surg Oncol*. 2010;8(1):1–7. doi:10.1186/1477-7819-8-72
253. Van Driel WJ, Koole SN, Sikorska K, et al. Hyperthermic intraperitoneal chemotherapy in ovarian cancer. *New Engl J Med*. 2018;378(3):230–240. doi:10.1056/NEJMoa1708618
254. Pawlik A, Nowak JM, Grzanka D, Gackowska L, Michalkiewicz J, Grzanka A. Hyperthermia induces cytoskeletal alterations and mitotic catastrophe in p53-deficient H1299 lung cancer cells. *Acta Histochem*. 2013;115(1):8–15. doi:10.1016/j.acthis.2012.02.006
255. Dolan EB, Haugh MG, Voisin MC, Tallon D, McNamara LM. Thermally induced osteocyte damage initiates a remodelling signaling cascade. *PLoS One* 2015;10(3). doi:10.1371/journal.pone.0119652
256. Alqhtani N, Alenazi A, Nasyam FA, Mehaji S. Influencing effect of heat therapy on osteoblasts growth and differentiation following treatment with bone antiresorptive drugs-an in vitro study. *J Young Pharm*. 2019;11(4):395. doi:10.5530/jyp.2019.11.81
257. Vos LM, Aronson SL, van Driel WJ, et al. Translational and pharmacological principles of hyperthermic intraperitoneal chemotherapy for ovarian cancer. *Best Pract Res Clin Obstet Gynaecol*. 2022;78:86.
258. Salunkhe A, Khot V, Patil S, Tofail SA, Bauer J, Thorat ND. MRI guided magneto-chemotherapy with high-magnetic-moment iron oxide nanoparticles for cancer theranostics. *ACS Appl Bio Mater*. 2020;3(4):2305–2313. doi:10.1021/acsabm.0c00077
259. Thorat ND, Bohara RA, Tofail SA, et al. Superparamagnetic gadolinium ferrite nanoparticles with controllable curie temperature–cancer theranostics for MR-imaging-guided magneto-chemotherapy. *Eur J Inorg Chem*. 2016;2016(28):4586–4597.
260. Wang N, Cheng X, Li N, Wang H, Chen H. Nanocarriers and their loading strategies. *Adv Healthcare Mater*. 2019;8(6):1801002. doi:10.1002/adhm.201801002
261. Peigneux A, Oltolina F, Colangelo D, et al. Functionalized biomimetic magnetic nanoparticles as effective nanocarriers for targeted chemotherapy. *Part Part Syst Charact*. 2019;36(6):1900057.
262. Ullah S, Seidel K, Türkkan S, et al. Macrophage entrapped silica coated superparamagnetic iron oxide particles for controlled drug release in a 3D cancer model. *J Control Release*. 2019;294:327–336. doi:10.1016/j.jconrel.2018.12.040
263. Cho H-Y, Lee T, Yoon J, et al. Magnetic oleosome as a functional lipophilic drug carrier for cancer therapy. *ACS Appl Mater Interfaces*. 2018;10(11):9301–9309. doi:10.1021/acsami.7b19255
264. Christodoulou E, Nerantzaki M, Nanaki S, et al. Paclitaxel magnetic core–shell nanoparticles based on poly (Lactic acid) semitelechelic novel block copolymers for combined hyperthermia and chemotherapy treatment of cancer. *Pharmaceutics*. 2019;11(5):213. doi:10.3390/pharmaceutics11050213
265. Dutta B, Checker S, Barick K, Salunke H, Gota V, Hassan P. Malic acid grafted Fe3O4 nanoparticles for controlled drug delivery and efficient heating source for hyperthermia therapy. *J Alloys Compd*. 2021;883:160950. doi:10.1016/j.jallcom.2021.160950
266. Hovhannisyan V, Siposova K, Musatov A, Chen S-J. Development of multifunctional nanocomposites for controlled drug delivery and hyperthermia. *Sci Rep*. 2021;11(1):1–10. doi:10.1038/s41598-021-84927-x
267. Jang J-t, Jeoung JW, Park JH, et al. Effects of recovery time during magnetic nanofluid hyperthermia on the induction behavior and efficiency of heat shock proteins 72. *Sci Rep*. 2017;7(1):1–9. doi:10.1038/s41598-017-14348-2
268. Hatamie S, Balasi ZM, Ahadian MM, Mortezazadeh T, Shams F, Hosseinzadeh S. Hyperthermia of breast cancer tumor using graphene oxide-cobalt ferrite magnetic nanoparticles in mice. *J Drug Deliv Sci Technol*. 2021:102680. doi:10.1016/j.jddst.2021.102680
269. Mngadi S, Singh M, Mokhosi S. PVA coating of ferrite nanoparticles triggers pH-responsive release of 5-fluorouracil in cancer cells. *J Polym Eng*. 2021:597–606. doi:10.1515/polyeng-2020-0271
270. Thorat ND, Bohara RA, Noor MR, Dhamecha D, Soulimane T, Tofail SA. Effective cancer theranostics with polymer encapsulated superparamagnetic nanoparticles: combined effects of magnetic hyperthermia and controlled drug release. *ACS Biomater Sci Eng*. 2017;3(7):1332–1340. doi:10.1021/acsbiomaterials.6b00420
271. Chen J, Liu J, Hu Y, Tian Z, Zhu Y. Metal-organic framework-coated magnetite nanoparticles for synergistic magnetic hyperthermia and chemotherapy with pH-triggered drug release. *Sci Technol Adv Mate*. 2019;20(1):1043–1054. doi:10.1080/14686996.2019.1682467
272. Chen B, Xing J, Li M, Liu Y, Ji M. DOX@ ferumoxytol-medical chitosan as magnetic hydrogel therapeutic system for effective magnetic hyperthermia and chemotherapy in vitro. *Colloids Surf B Biointerfaces*. 2020;190:110896. doi:10.1016/j.colsurfb.2020.110896
273. Tapeinos C, Marino A, Battaglini M, et al. Stimuli-responsive lipid-based magnetic nanovectors increase apoptosis in glioblastoma cells through synergic intracellular hyperthermia and chemotherapy. *Nanoscale*. 2019;11(1):72–88. doi:10.1039/C8NR05520C
274. Norouzi M, Yathindranath V, Thliveris JA, Kopec BM, Siahaan TJ, Miller DW. Doxorubicin-loaded iron oxide nanoparticles for glioblastoma therapy: a combinational approach for enhanced delivery of nanoparticles. *Sci Rep*. 2020;10(1):1–18. doi:10.1038/s41598-020-68017-y
275. Mannu R, Karthikeyan V, Velu N, et al. Polyethylene glycol coated magnetic nanoparticles: hybrid nanofluid formulation, properties and drug delivery prospects. *Nanomaterials*. 2021;11(2):440. doi:10.3390/nano11020440
276. Sasikala ARK, Unnithan AR, Yun Y-H, Park CH, Kim CS. An implantable smart magnetic nanofiber device for endoscopic hyperthermia treatment and tumor-triggered controlled drug release. *Acta Biomater*. 2016;31:122–133. doi:10.1016/j.actbio.2015.12.015

277. Radmansouri M, Bahmani E, Sarikhani E, Rahmani K, Sharifianjazi F, Irani M. Doxorubicin hydrochloride-loaded electrospun chitosan/cobalt ferrite/titanium oxide nanofibers for hyperthermic tumor cell treatment and controlled drug release. *Int J Biol Macromol*. 2018;116:378–384. doi:10.1016/j.ijbiomac.2018.04.161
278. Jang Jt, Lee J, Seon J, et al. Giant magnetic heat induction of magnesium-doped γ-Fe2O3 superparamagnetic nanoparticles for completely killing tumors. *Adv Mater*. 2018;30(6):1704362. doi:10.1002/adma.201704362
279. Moorthy MS, Bharathiraja S, Manivasagan P, Lee KD, Oh J. Crown ether triad modified core–shell magnetic mesoporous silica nanocarrier for pH-responsive drug delivery and magnetic hyperthermia applications. *New J Chem*. 2017;41(19):10935–10947. doi:10.1039/C7NJ02432K
280. Sadr SH, Davaran S, Alizadeh E, Salehi R, Ramazani A. PLA-based magnetic nanoparticles armed with thermo/pH responsive polymers for combination cancer chemotherapy. *J Drug Deliv Sci Technol*. 2018;45:240–254. doi:10.1016/j.jddst.2018.03.019
281. Garanina A, Kireev I, Zhironkina O, et al. Long-term live cells observation of internalized fluorescent Fe@ C nanoparticles in constant magnetic field. *J Nanobiotechnology*. 2019;17(1):1–10. doi:10.1186/s12951-019-0463-5
282. Huang HS, Hainfeld JF. Intravenous magnetic nanoparticle cancer hyperthermia. *Int J Nanomedicine*. 2013;8:2521. doi:10.2147/IJN.S43770
283. Liu XL, Yang Y, Ng CT, et al. Magnetic vortex nanorings: a new class of hyperthermia agent for highly efficient in vivo regression of tumors. *Adv Mater*. 2015;27(11):1939–1944. doi:10.1002/adma.201405036
284. Oltolina F, Peigneux A, Colangelo D, et al. Biomimetic magnetite nanoparticles as targeted drug nanocarriers and mediators of hyperthermia in an experimental cancer model. *Cancers*. 2020;12(9):2564. doi:10.3390/cancers12092564
285. Dabbagh A, Hedayatnasab Z, Karimian H, et al. Polyethylene glycol-coated porous magnetic nanoparticles for targeted delivery of chemotherapeutics under magnetic hyperthermia condition. *Int J Hyperthermia*. 2019;36(1):104–114. doi:10.1080/02656736.2018.1536809
286. Albarqi HA, Wong LH, Schumann C, et al. Biocompatible nanoclusters with high heating efficiency for systemically delivered magnetic hyperthermia. *ACS nano*. 2019;13(6):6383–6395. doi:10.1021/acsnano.8b06542
287. Parekh K, Bhardwaj A, Jain N. Preliminary in-vitro investigation of magnetic fluid hyperthermia in cervical cancer cells. *J Magn Magn Mater*. 2020;497:166057. doi:10.1016/j.jmmm.2019.166057
288. Zelepukin IV, Yaremenko AV, IvanovIN, et al. Long-term fate of magnetic particles in mice: a comprehensive study. *Acs Nano*. 2021;15(7):11341–11357. doi:10.1021/acsnano.1c00687
289. Zelepukin IV, Yaremenko AV Yuryev MV, et al. Fast processes of nanoparticle blood clearance: comprehensive study. *J Control Release*. 2020;326:181–191. doi:10.1016/j.jconrel.2020.07.014
290. Wang J, Chen Y, Chen B, et al. Pharmacokinetic parameters and tissue distribution of magnetic Fe3O4 nanoparticles in mice. *Int J Nanomedicine*. 2010;5:861. doi:10.2147/IJN.S13662
291. Gustafson HH, Holt-Casper D, Grainger DW, Ghandehari H. Nanoparticle uptake: the phagocyte problem. *Nano Today* 2015;10(4):487–510. doi:10.1016/j.nantod.2015.06.006
292. Tregubov A, Sokolov I, Babenyshev A, Nikitin P, Cherkasov V, Nikitin M. Magnetic hybrid magnetite/metal organic framework nanoparticles: facile preparation, post-synthetic biofunctionalization and tracking in vivo with magnetic methods. *J Magn Magn Mater*. 2018;449:590–596. doi:10.1016/j.jmmm.2017.10.070
293. Van de Walle A, Plan Sangnier A, Abou-Hassan A, et al. Biosynthesis of magnetic nanoparticles from nano-degradation products revealed in human stem cells. *Proc Natl Acad Sci U S A*. 2019;116(10):4044–4053.
294. Hall JE, Hall ME. *Guyton and Hall Textbook of Medical Physiology e-Book*. Elsevier Health Sciences; 2020.
295. Ruiz A, Hernandez Y, Cabal C, et al. Biodistribution and pharmacokinetics of uniform magnetite nanoparticles chemically modified with polyethylene glycol. *Nanoscale*. 2013;5(23):11400–11408. doi:10.1039/c3nr01412f
296. Sangnier AP, Van de Walle AB, Curcio A, et al. Impact of magnetic nanoparticle surface coating on their long-term intracellular biodegradation in stem cells. *Nanoscale*. 2019;11(35):16488–16498. doi:10.1039/C9NR05624F
297. Albanese A, Tang PS, Chan WC. The effect of nanoparticle size, shape, and surface chemistry on biological systems. *Annu Rev Biomed Eng*. 2012;14:1–16. doi:10.1146/annurev-bioeng-071811-150124
298. Kudr J, Haddad Y, Richtera L, et al. Magnetic nanoparticles: from design and synthesis to real world applications. *Nanomaterials*. 2017;7(9):243. doi:10.3390/nano7090243
299. Banerjee A, Qi J, Gogoi R, Wong J, Mitragotri S. Role of nanoparticle size, shape and surface chemistry in oral drug delivery. *J Control Release*. 2016;238:176–185. doi:10.1016/j.jconrel.2016.07.051
300. Gul S, Khan SB, Rehman IU, Khan MA, Khan M. A comprehensive review of magnetic nanomaterials modern day theranostics. *Front Mater*. 2019;6:179. doi:10.3389/fmats.2019.00179
301. Lee MJ-E, Veiseh O, Bhattarai N, et al. Rapid pharmacokinetic and biodistribution studies using cholorotoxin-conjugated iron oxide nanoparticles: a novel non-radioactive method. *PLoS One*. 2010;5(3):e9536. doi:10.1371/journal.pone.0009536
302. Rahman A, Likius D, Uahengo V, Iqbaluddin S. A mini review highlights on the application of nano-materials for Kidney disease: a key development in medicinal therapy. *Nephrol Renal Dis*. 2017;2(2):1–6. doi:10.15761/NRD.1000121
303. Perez M, Maiguy-Foinard A, Barthélémy C, Décaudin B, Odou P. Particulate matter in injectable drugs: evaluation of risks to patients. *Pharm Technol Hosp Pharm*. 2016;1(2):91–103. doi:10.1515/pthp-2016-0004
304. Levy M, Luciani N, Alloyeau D, et al. Long term in vivo biotransformation of iron oxide nanoparticles. *Biomaterials*. 2011;32(16):3988–3999. doi:10.1016/j.biomaterials.2011.02.031
305. Bilyy R, Bila G, Vishchur O, Vovk V, Herrmann M. Neutrophils as main players of immune response towards nondegradable nanoparticles. *Nanomaterials*. 2020;10(7):1273. doi:10.3390/nano10071273
306. Liu JF, Jang B, Issadore D, Tsourkas A. Use of magnetic fields and nanoparticles to trigger drug release and improve tumor targeting. *Wiley Interdiscip Rev Nanomed Nanobiotechnol*. 2019;11(6):e1571. doi:10.1002/wnan.1571
307. Marín T, Montoya P, Arnache O, Pinal R, Calderón J. Development of magnetite nanoparticles/gelatin composite films for triggering drug release by an external magnetic field. *Mater Des*. 2018;152:78–87. doi:10.1016/j.matdes.2018.04.073
308. Liu Y-L, Chen D, Shang P, Yin D-C. A review of magnet systems for targeted drug delivery. *J Control Release*. 2019;302:90–104. doi:10.1016/j.jconrel.2019.03.031
309. Heldin C-H, Rubin K, Pietras K, Östman A. High interstitial fluid pressure—an obstacle in cancer therapy. *Nat Rev Cancer*. 2004;4(10):806–813. doi:10.1038/nrc1456

310. Barua S, Mitragotri S. Challenges associated with penetration of nanoparticles across cell and tissue barriers: a review of current status and future prospects. *Nano Today*. 2014;9(2):223–243. doi:10.1016/j.nantod.2014.04.008
311. Yuan F, Dellian M, Fukumura D, et al. Vascular permeability in a human tumor xenograft: molecular size dependence and cutoff size. *Cancer Res*. 1995;55(17):3752–3756.
312. Danhier F, Feron O, Préat V. To exploit the tumor microenvironment: passive and active tumor targeting of nanocarriers for anti-cancer drug delivery. *J Control Release*. 2010;148(2):135–146. doi:10.1016/j.jconrel.2010.08.027
313. Wang J, Mao W, Lock LL, et al. The role of micelle size in tumor accumulation, penetration, and treatment. *ACS nano*. 2015;9(7):7195–7206. doi:10.1021/acsnano.5b02017
314. Ruan S, Cao X, Cun X, et al. Matrix metalloproteinase-sensitive size-shrinkable nanoparticles for deep tumor penetration and pH triggered doxorubicin release. *Biomaterials*. 2015;60:100–110. doi:10.1016/j.biomaterials.2015.05.006
315. Shapiro B, Kulkarni S, Nacev A, Muro S, Stepanov PY, Weinberg IN. Open challenges in magnetic drug targeting. *Wiley Interdiscip Rev Nanomed Nanobiotechnol*. 2015;7(3):446–457. doi:10.1002/wnan.1311
316. Liu JF, Lan Z, Ferrari C, et al. Use of oppositely polarized external magnets to improve the accumulation and penetration of magnetic nanocarriers into solid tumors. *ACS nano*. 2019;14(1):142–152. doi:10.1021/acsnano.9b05660
317. Zhou Z, Shen Z, Chen X. Tale of two magnets: an advanced magnetic targeting system. *ACS nano*. 2019;14(1):7–11. doi:10.1021/acsnano.9b06842
318. Benos L, Ninos G, Polychronopoulos ND, Exomanidou M-A, Sarris I. Natural convection of blood–magnetic iron oxide bio-nanofluid in the context of hyperthermia treatment. *Computation*. 2022;10(11):190. doi:10.3390/computation10110190
319. Tehrani MH, Soltani M, Moradi Kashkooli F, Mahmoudi M, Raahemifar K. Computational modeling of combination of magnetic hyperthermia and temperature-sensitive liposome for controlled drug release in solid tumor. *Pharmaceutics*. 2021;14(1):35. doi:10.3390/pharmaceutics14010035
320. Lemke A-J, von Pilsach M-IS, Lübbe A, Bergemann C, Riess H, Felix R. MRI after magnetic drug targeting in patients with advanced solid malignant tumors. *Eur Radiol*. 2004;14(11):1949–1955. doi:10.1007/s00330-004-2445-7
321. Wust P, Gneveckow U, Wust P, et al. Magnetic nanoparticles for interstitial thermotherapy–feasibility, tolerance and achieved temperatures. *Int J Hyperthermia*. 2006;22(8):673–685. doi:10.1080/02656730601106037